Commission of the European Communities

nuclear science and technology

The location of uranium in source rocks and sites of secondary deposition at the Needle's Eye natural analogue site, Dumfries and Galloway

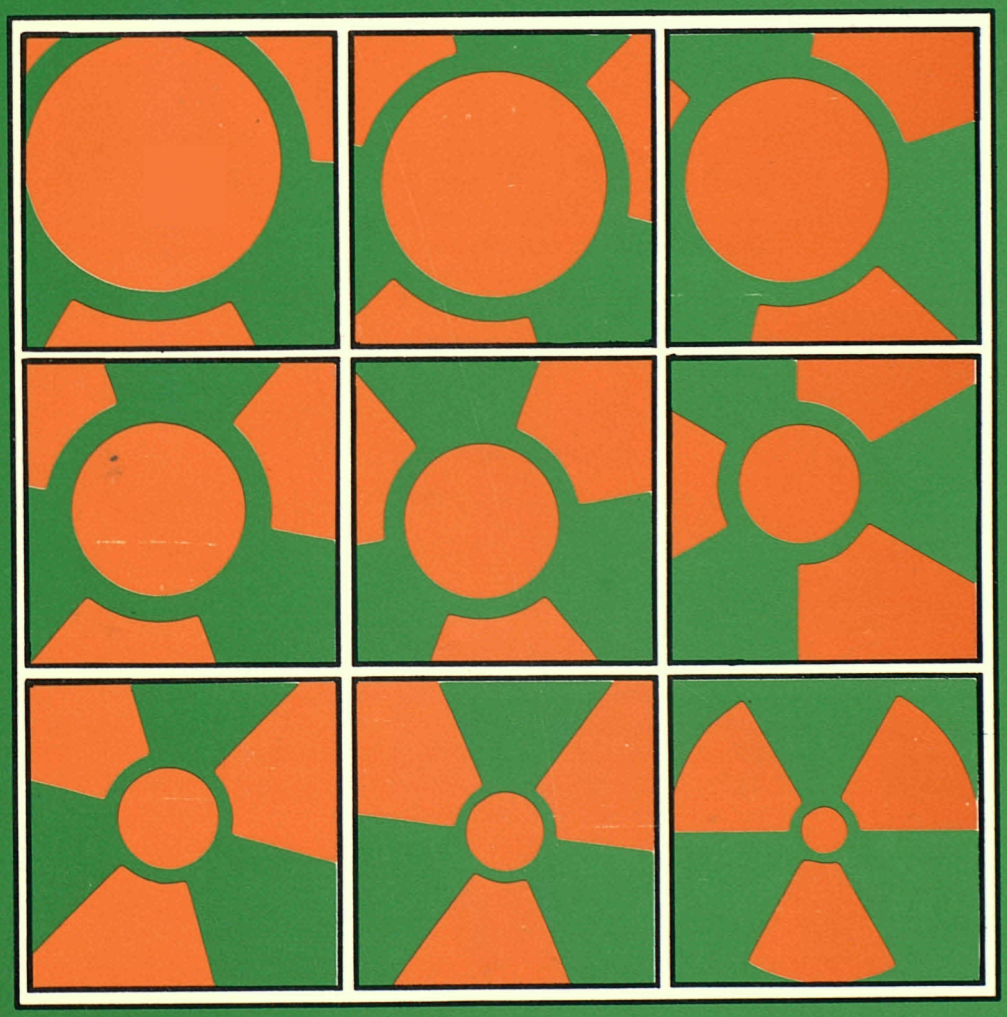

Report

EUR 13279 EN

Commission of the European Communities

nuclear science and technology

The location of uranium in source rocks and sites of secondary deposition at the Needle's Eye natural analogue site, Dumfries and Galloway

I. R. Basham,[1] A. E. Milodowski,[2]
E. K. Hyslop,[1] J.M. Pearce[2]

British Geological Survey
[1] Edinburgh,
United Kingdom
[2] Keyworth, Nottingham NG12 5GG,
United Kingdom

Topical report

Work carried out under cost-sharing contract
No FI1W/0073/UK with the European Atomic Energy Community,
in the framework of its third R&D programme on
'Management and storage of radioactive waste', Part A, Task 4
'Geological disposal studies'

Directorate-General
Science, Research and Development

1991

EUR 13279 EN

Published by the
COMMISSION OF THE EUROPEAN COMMUNITIES
Directorate-General
Telecommunications, Information Industries and Innovation
L-2920 Luxembourg

Cataloguing data can be found at the end of this publication

Luxembourg: Office for Official Publications of the European Communities, 1991

ISBN 92-826-2421-8 Catalogue number: CD-NA-13279-EN-C

Printed in Belgium

PREFACE

The British Geological Survey (BGS) has been conducting a coordinated research programme at the Needle's Eye natural analogue site in Dumfries and Galloway District, southwest Scotland. This work on a natural radioactive geochemical system has been carried out with the aim of improving our confidence in using predictive models of radionuclide migration in the geosphere. It has involved collaboration with the Scottish Universities Research and Reactor Centre, East Kilbride, for natural decay series (U/Th) analytical work, and with the Ecole des Mines de Paris (Centre d'Informatique Géologique), Fontainebleau, for geochemical modelling. The natural analogue work jointly carried out has been supported by the Department of the Environment from July 1986 to March 1989 and by the Commission of the European Communities from July 1988 to September 1989 under the CEC shared-cost action MIRAGE II Project.

This report is one of a series being produced from this effort and is concerned with the mineralogical characterisation of the distribution of uranium in the 'primary' sites of hydrothermal mineral veins associated with the Criffel Granodiorite and its contact metamorphic envelope of Silurian hornfels, and in the sites of secondary redeposition in the Quaternary estuarine sediments of the Solway Firth. Other reports listed below give further details of the programme.

Needle's Eye reports and papers:

[1] HOOKER, P.J., MacKENZIE, A.B., SCOTT, R.D., IVANOVICH, M., BALL, T.K., BASHAM, I.R., BLOODWORTH, A.J., ROBERTS, P.D. : Natural analogues of radionuclide migration: reconnaissance study of sites (May 1985-March 1986). British Geological Survey Report FLPU 86-6 (1986).

[2] HOOKER, P.J., CHAPMAN, N.A., MacKENZIE, A.B., SCOTT, R.D., IVANOVICH, M. in: Natural Analogues in Radioactive Waste Disposal (B. Come and N.A. Chapman, Eds) CEC EUR 11037 EN (Graham & Trotman), 104-115 (1987).

[3] ROBERTS, P.D., BALL, T.K., HOOKER, P.J., MILODOWSKI, A.E. : A uranium geochemical study at the natural analogue site of Needle's Eye, SW Scotland. Mat. Res. Soc. Symp. Proc. 127, 933-940 (1989).

[4] HIGGO, J.J.W., FALCK, W.E., HOOKER, P.J. : Sorption studies of uranium in sediment-groundwater systems from the natural analogue sites of Needle's Eye and Broubster. British Geological Survey Technical Report WE/89/40 (1989).

[5] SOUBEYRAN, R., LEDOUX, E., de MARSILY, G. : Modélisation du transfert d''analogues' naturels. Ecole des Mines de Paris (C.I.G.) progress report to 31.12.87, LHM/RD/88/11, 42pp (in French) (1988).

[6] DOUBLET, R., JAMET, Ph., SOUBEYRAN, R. : Hydrogéochimie du site de Needle's Eye - Premiere interprétations. Ecole des Mines de Paris (C.I.G.) progress report to 30.6.88, LHM/RD/88/59, 34pp (in French) (1988). Also in English as British Geological Survey Technical Report WE/89/55.

[7] JAMET, Ph., LACHASSAGNE, P., DOUBLET, R. : Modélisation hydrogéochimique du site de Needle's Eye. Ecole des Mines de Paris (C.I.G.) progress report to 31.12.88, LHM/RD/89/66, 38pp (in French) (1989).

CONTENTS

FIGURES:

EXECUTIVE SUMMARY

Supported by the Department of the Environment from July 1986 to March 1989 and by the Commission of the European Communities from July 1988 to September 1989 under the shared-cost action MIRAGE II Project, the British Geological Survey (BGS) has been conducting a number of investigations of locations where natural analogues of radionuclide migration can be recognised. The purpose of the research is to describe the processes of movement of uranium, thorium and rare earth elements (REE) in sediments, in order to provide data which can be used in modelling and testing applications of the CHEMVAL thermodynamic database and of transport codes such as CHEMTARD. Testing with real geological situations in this way can create confidence in the use of such codes as predictors of radionuclide transport in performance assessments of radioactive waste repositories.

The Needle's Eye site in the district of Dumfries and Galloway in southwest Scotland was selected for study in the natural analogue programme on the basis of a detailed account, published in 1966 by BGS staff, which demonstrated the presence of a highly leachable source of uranium in pitchblende mineralization in ancient sea cliffs, and radiometric evidence of dispersion into the silty sediments of mudflats below. This report presents mineralogical and petrological results obtained from a variety of samples from the site, examined with the objective of establishing the mineralogical and geochemical character of uranium distribution in both the "source-term" and the "sink" locations.

Detailed determination of the distribution and mineralogical character of uranium in the "source-term" and in sites of secondary deposition is required in order to assess susceptibility to remobilisation by weathering and leaching in the former and the retarding and concentrating mechanisms operative in the latter. This has been accomplished by the integration of a variety of mineralogical methods. Autoradiographic and uranium fission track techniques have been used to locate and quantify uranium in levels ranging from a few to several hundred parts per million (ppm), identification of the host phases being made subsequently by optical and scanning electron microscopy. Samples of the vein mineralization and of the Late Caledonian Criffel granodiorite and hornfelsed Silurian metasediments which form the host rocks were collected directly from exposures in the cliff area. Undisturbed samples of soils and unconsolidated Quaternary estuarine and intertidal sediments from the mudflats at the base of the cliffs were collected from two excavated pits, sited to lie immediately over postulated extensions of the pitchblende vein. The principal forms of specimens examined were conventional polished thin sections, prepared directly from the rock and vein samples, and following non-disruptive impregnation of the undisturbed sediment samples. The latter were also studied as large (10 by 5 cm) sections in

order to assess fully the complete sediment profile. Preliminary alpha particle autoradiography of these sections enabled a realistic appraisal of the overall distribution of radioelement concentrations to be made prior to detailed evaluation of individual locations.

The investigation has confirmed that the most important location of readily mobilised uranium in the cliff section is the uraninite (variety pitchblende) in the polymetallic-carbonate breccia veins. Contemporary weathering is seen to be active in the redistribution of uranium from this source by the abundance of secondary uranium minerals, mainly arsenates and silicate-hydrates, found within the vein and related wall-rocks. Together with uranium absorbed from groundwater by ferruginous weathering products of sulphides in the veins and iron-rich silicates in the host-rocks, these uranium phases present a minor, but widespread ancillary source of uranium. Similar so-called "secondary" uranium minerals have been identified in intimate association with the ore minerals in the vein and are considered to have formed as part of the paragenesis, the polymetallic character of which is reflected in a variety of sulphides, arsenides etc. These are also relatively unstable in the supergene environment, becoming oxidised and giving rise to a large number of complex secondary minerals. The ability of hexavalent uranium to combine with a wide range of cations and anionic complexes (eg phosphate, arsenate, vanadate, silicate hydrate) results in redeposition of uranium as secondary minerals in close proximity to source. The composition of these minerals may vary within a short distance, reflecting local availability of formative elements and often two or more secondary minerals occur together in close textural association. This study has recognised several such secondary uranium minerals within the veins themselves and in fractures in the adjacent wallrocks, including several not previously recorded from the site.

Globular hydrocarbon is common in the veins but this study, in contrast to other reported research, has shown that it does not, in itself, contain labile uranium and, as it is considered to be relatively stable in the present supergene environment, release of significant uranium from any discrete included uraninite is thought unlikely.

Both the granodiorite and the hornfelsed siltstone host rocks have been affected by wall-rock alteration. Pervasive fine mineral veining has created a halo of primary metal enrichment around the main "source-term" vein and uranium might be mobilised from that zone to a lesser degree. Perhaps more important is the recognition of pervasive potassic alteration and feldspar development in the granodiorite which appears to have resulted in the alteration, of uranium-bearing primary accessory minerals and remobilisation and redeposition of uranium in the granodiorite as fine grained uranium-thorium-REE silicates and phosphates. Together with metamictised primary thorium and REE minerals, these present possible "source-terms"

for modelling mobilisation and transport of the thorium-series and rare earth analogue elements and are worthy of further study in this respect. Limited preliminary analysis of granodiorite some distance from the Needle's Eye vein indicates that these features may be present on a more regional basis. In any case, modelling of the transport of uranium series elements in the cliff waters should not exclude the possibility of input from the cliff rocks, additional to that from the vein pitchblende.

Study of samples from profiles in the Quaternary sediments and overlying peaty soils has shown that uranium being carried seawards by groundwaters from the cliff area has been effectively retarded by organic matter. Fission track techniques have demonstrated convincingly the strong correlation of uranium with both semi-amorphous, humified (peaty) organic matter in the near-surface horizons and discrete plant root structures preserved in the lower parts of the sediment pile. Local concentrations of several hundreds ppm uranium occur in the peats, mainly around open, oxygenated root channels. Much higher levels are attained within the plant structures, apparently in cell material related to the water uptake system thus suggesting accumulation by the plant while living. Further study of live plant material from the site is needed to confirm this supposition which, if correct, would indicate that the transport and fixation mechanisms related to the soil-forming processes active on the sediments near the bottom of the pile were comparable to those of the present-day.

Of considerable scientific interest and significance to transport modelling in this organic-rich environment, is the evidence found of the effectiveness of micro-organisms associated with exposed fracture surfaces on hydrocarbon in accumulating uranium and other metallic elements mobilised in groundwaters from the mineral veins. The mineralizing capability of bacteria is shown to be potentially a strong concentrating mechanism in the soil regime at this site and further investigation of its extent as a retardant is warranted.

1. INTRODUCTION

The British Geological Survey (BGS) has been conducting a number of investigations of natural radioactive geochemical systems in order to obtain data to be used in testing the application of various thermodynamic databases and equilibrium speciation codes in modelling migration and retardation mechanisms of radionuclide transport. The uranium vein-type mineralization at Needle's Eye, near Dalbeattie in southwest Scotland provides a suitable focus for such a study. This report presents mineralogical and petrological results obtained from a variety of samples from the site, examined with the objective of establishing the mineralogical and geochemical character of uranium distribution in both the "source-term" and the "sink" locations in the natural analogue model. As the principal mineralization is of uranium, accompanied by a number of metallic sulphides, less attention has been paid initially to the distribution of other analogue elements. However, the study has shown that thorium and rare earth elements are present in associated host-rocks at the site. Some preliminary information on the occurrence of these is included in this report, which builds upon and elaborates the earlier provisional account of the source-term and sites of secondary uranium accumulation given by Basham and Hyslop (1989). Data from this mineralogical and petrological study will be used to assist interpretation of chemical, radiospectrometric, hydrogeochemical, hydrogeological and other data being used in the assessment of geochemical models and coupled-transport codes.

2. GEOLOGICAL SETTING

2.1 SITE LOCATION

The Needle's Eye Natural Analogue site (National Grid Reference NX 915 562) is located on the north coast of the Solway Firth about 9km southeast of Dalbeattie in the district of Dumfries and Galloway in southwest Scotland (Figure 1). The area of interest is part of a nature reserve and a site of special scientific interest administered by the Scottish Wildlife Trust. It is bounded to the south by the tidal creek of the Southwick Water and to the north by the clifftop at Nether Clifton (Plate 1). Most of the site rests on relatively low-lying ground between 2-6m AOD developed on the estuarine/intertidal mudflats of the Mersehead Sands and is subject to inundation during spring, neap or storm tides. However, the cliffs to the north of the site rise steeply to an elevation between 26-45m AOD and further inland the ground continues to rise steeply (Plate 2). The site takes its name from a natural arch formed by Quaternary coastal erosion.

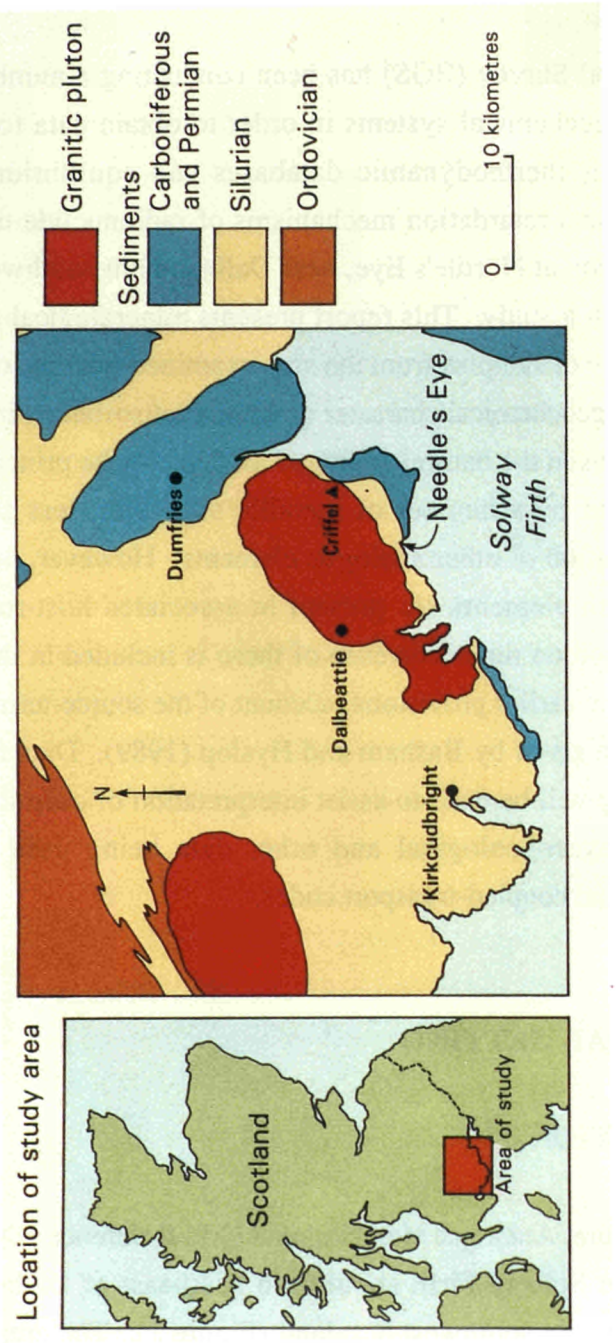

Figure 1 Regional geology, showing location of the Needle's Eye site.

PLATE 1. Photograph looking east over the Mersehead estuarine/ intertidal mudflats and the Southwick Water tidal creek on the southern boundary of the Needle's Eye research site, showing the ancient cliff line which fringes the mudflats to the north. Note Carboniferous limestone exposed in the creek. However, the cliffs to the north of the site rise steeply to an elevation between 26-45m AOD and further inland the ground continues to rise steeply (Plate 2). The site takes its name from a natural arch formed by Quaternary coastal erosion.

PLATE 2.Photograph of the Needle's Eye research site looking north from Southwick Water, showing the ancient sea cliff containing the mineralization above the vegetated mudflats; a small intertidal creek drains the site.

PLATE 3 Detail of the vein mineralization exposed in the cliff face which was sampled for this study. The near vertical carbonate breccia vein (5-10cm wide) is bounded on the right by highly sheared hornfels and on the left by a tongue of more massive granodiorite.

2.2 SOLID GEOLOGY

The regional geological setting of the Needle's Eye site is shown in Figure 1 and the local geology of the site together with the sampling locations of materials considered in this report summarised in Figure 2. The site is located close to the contact zone of the Criffel Granodiorite and Silurian metasediments of the Southern Uplands accretionary complex. The geology of the site has been described in detail by Miller and Taylor (1966) and is only summarised here.

The Criffel pluton is a Late Caledonian intrusive complex (397 ± 2my; Halliday *et al*, 1980) which intrudes and was responsible for the thermal metamorphism of the Silurian sediments, is concentrically zoned from an outer metaluminous hornblende granodiorite to a core of peraluminous muscovite granite. Rare earth element (REE) zonation has also been recorded (Stephens *et al*, 1985), total REE contents decreasing progressively towards the centre. A series of related porphyrite or porphyry dykes occurs in clusters, mainly along the southeast margin of the pluton, trending generally northwesterly (Phillips *et al*, 1981).

The intruded Silurian sediments comprise mainly siltstones and greywackes and show a distinct hornfelsed aureole within which most of the mineralization is concentrated. A major east-west fault brings these Lower Palaeozoic rocks into juxtaposition with downthrown Carboniferous sediments (interbedded limestones and shales) to the south. This fault skirts the base of the cliffs and is generally responsible for the long straight coastal feature. Shearing, brecciation and silicification parallel to this fault affects the Silurian, with further tectonic disturbance resulting from the development of cross-faults.

Polymetallic mineralization occurs within a number of steeply inclined veins (Plate 3) in the northwest cross-fractures cutting the northeasterly coastal fault. Mineralization rarely occurs, however, at the fracture-fault intersections and the veins reach their maximum development in the hornfels between 10-30 metres north of the fault. The veins occur in clusters, with intervening barren zones, mainly where the fault changes direction and where feather faults branch off the main structure. The greatest intensity of vein mineralization is developed where the fault approaches the granodiorite contact and is often concentrated along the margins of acidic dykes, although the implied structural relationship has not been established. Limited mineralization has been reported from the Carboniferous sediments, which are presumed to have been relatively soft and acted as a seal to the migration of mineralizing fluids in the fractured hornfels (Miller and Taylor, 1966). However, Miller and Taylor established that at least one vein containing uranium mineralization continues under the mudflat sediments at Needle's Eye and crosses into the Carboniferous rocks.

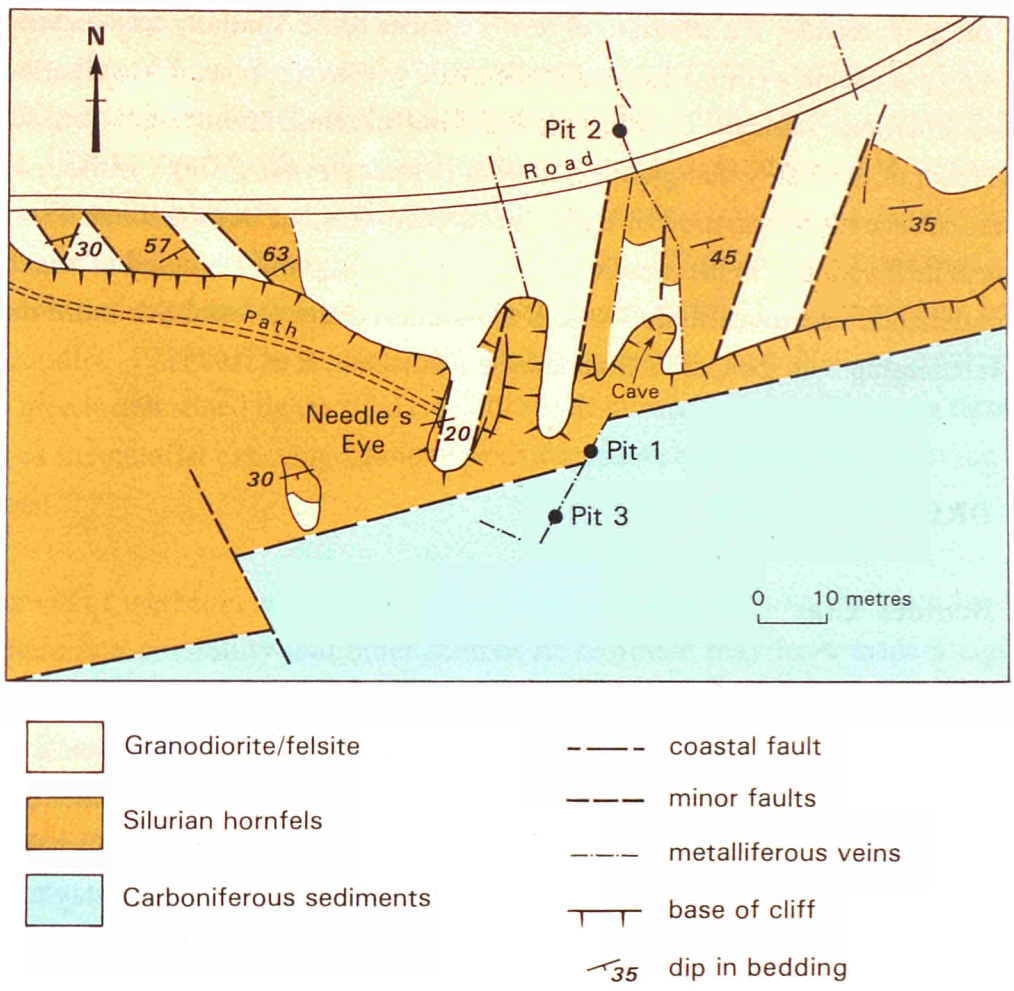

Figure 2: Geology of the Needle's Eye site, showing pit and sample locations (modified after Miller and Taylor, 1966).

Uraninite (variety pitchblende) from the veins has been dated as 185±20my and the complete mineralization episode is believed to have occurred between that date and the Lower Carboniferous (Miller and Taylor, 1966). Despite the considerably younger Triassic-Jurassic age of the pitchblende, the uranium deposits appear to be spatially associated with the Caledonian pluton and a comparison might be made with veins in southwest England where age determinations indicate intermittent uranium mineralization continuing long after emplacement of the Hercynian granite batholith (Darnley *et al*, 1965). In both instances, however, no recent confirmation of these pitchblende ages has been made and some doubt exists as to their validity. In the present case, the precise origin of the uranium mineralization is not understood and much more work is required in order to establish more than just a spatial relationship with the Criffel Granodiorite (Gallagher, *et al*, 1971).

2.3 DRIFT GEOLOGY

2.3.1 Boulder Clay

During the last Pleistocene glaciation this area was completely submerged beneath a thick sheet of ice that covered most of Scotland (Goodlet, 1970). These ice sheets deposited extensive ground moraine or boulder clay over much of the region. This boulder clay occurs as undulating sheets on the lower hill slopes, thickening into the valleys and forming poorly-defined terraces along the larger water courses. The nature of the boulder clay varies from place to place depending on the nature of the underlying bedrock. Thus on Palaeozoic sedimentary bedrock it usually has a matrix consisting of a tough, tenacious clay but in granitic areas it is more gritty and less cohesive (Goodlet, 1970). Much of the clay consists of locally derived material containing boulders from local granitic plutons and country rocks (Horne, 1896) and where the sources of these boulders have been determined they indicate transport from the north or northwest (Goodlet, 1970).

2.3.2 Estuarine and Intertidal Deposits

The bedrock at the base of the cliffs at Needle's Eye has been planed by post-glacial (Quaternary) marine erosion with the development of a wave-cut platform, sea-stacks and small caves in the cliffs (the formation of the natural arch of Needle's Eye being part of this process). Subsequent eustatic elevation of the land following post-glacial unloading of the ice has raised these features above the high tide mark, a common characteristic of the Solway Coast (eg Horne, 1896; Goodlet, 1970; Barnes, 1989). The erosion of these features by the sea in all likelihood was synchronous with the well-developed "25-feet" low raised beach

which forms a prominent and continuously traceable feature along the coast (Horne, 1896; Goodlet, 1970).

The deposits of the "25-feet" raised beach rest directly upon the eroded bedrock surface. They are particularly well-developed where streams have breached the precipitous coastline and extensive areas of beach deposit are found at the outfalls of all the main streams (Goodlet, 1970). The Needle's Eye site is situated at the edge of one such deposit which covers the foot of the ancient cliff-line and forms a prominent mudflat and saltmarsh about a mile wide, extending from Nether Clifton to Southerness. The deposits of this beach consist of well-stratified sand and fine gravel, associated in places with finely laminated estuarine clays (Goodlet, 1970). The southern limit of the Needle's Eye Natural Analogue site research area is delineated by the tidal creek of the Southwick Water which cuts through the deposits of the mudflat exposing Carboniferous limestone and shale bedrock in the base of the channel.

Whilst much of the sediment may be derived from streams draining the hinterland of the region there is a possibility that other sources of sediment may have made a significant contribution. Studies of the sedimentation pattern in the Irish Sea have shown that there is a very significant transport of sediment by tidal currents into the Solway Firth from the south and west (Cronan, 1969). Sediment derived from outside the region may therefore become incorporated in the deposits and as a result this may complicate any interpretation of the detrital components.

There is also evidence in the area that, at some time during the Quaternary, sea levels may have been lower than at present. Near Kirkcudbright Bay a peat bed with roots, hazel nuts and red deer remains, is exposed between tides and a similar peat bed overlain by finely laminated clays belonging to the low (25-feet) raised beach can be found near New Abbey (Goodlet, 1970). Traces of the associated beach deposits should therefore occur offshore in deeper water. Thus it would appear that there have been perturbations in the general relative rise of the land since the Pleistocene, with sea level reaching a lower level than the present day, then rising to form the "25-feet" raised beach, before falling to the present day level.

3. ANALYTICAL TECHNIQUES

3.1 SAMPLING

Samples of the granodiorite and hornfelsed Silurian country rocks, as well as the vein mineralization, were collected directly from exposures in the cliff area. Undisturbed samples of soils and unconsolidated drift sediments from the mudflats at the base of the cliffs were collected from two excavated pits (PIT 1 and PIT 3), sited to lie immediately over postulated extensions of the pitchblende vein (Figure 2). A further pit (PIT 2) was dug to intercept primary mineralization at the top of the cliff and will be discussed in a later report. Mineralisation was not encountered, the reason apparently being that a false position of the vein was indicated by the surface radiometric anomaly. Such displacement of a "false anomaly" is not uncommon and has probably arisen here as a result of the translocation of uranium by artesian groundwaters, now known to exist in the cliff area (Roberts *et al*, 1988), and its redeposition in sediments further away from its source.

The undisturbed soil/sediment samples were collected by pushing 5 x 10 cm aluminium soil boxes or "Kubiena tins" into the cleaned-up soil profile exposed in each soil pit. Once the soil boxes were completely let into the soil face they were excavated from behind, capped with lids and sealed with waterproof tape to prevent them from drying out during transport and storage. By this means a continuous vertical profile of the sediment at each site was preserved for petrographic characterisation, although it was not possible to sample undisturbed stoney soils in parts of the profiles where rock fragments prevented the insertion of the soil tins into the pit face. Samples for geochemical analysis were also taken over 10 cm intervals, corresponding with the soil box samples.

Full-size uncovered thin sections of the undisturbed soil samples were prepared in the Department of Soil Science, University of Aberdeen, following careful impregnation with epoxy-resin. The resin was emplaced in a slow but controlled manner by first displacing the porewater in the soil by a miscible organic solvent (acetone), then displacing the solvent by the epoxy resin solution. This technique reduced the damage to the sample that normally takes place due to shrinkage and disruption with simple drying techniques. After initial examination of the distribution of alpha particle tracks over the whole sample section area by autoradiography (Section 3.2), regions of particular interest were selected for the preparation of standard, smaller polished thin-sections for fission track work and subsequent detailed optical and scanning electron microscopy. Granodiorite, hornfels and vein samples were also prepared as polished thin sections and studied in a similar way.

3.2 AUTORADIOGRAPHY AND FISSION TRACK REGISTRATION

Uranium and thorium occur naturally in rocks in a great variety of host phases and in a wide range of concentrations (eg Basham *et al*, 1982). In any comprehensive mineralogical and geochemical study of radionuclide occurrence and distribution, the location of all possible hosts by charged particle track registration techniques is an essential precursor to evaluation by identification methods such as optical and electron microscopy. In this study, preliminary evaluation of the distribution of overall radioactivity was made by registration of natural alpha particle activity in polished thin sections in CR39 plastic, following the procedures described by Basham (1981). This was applied particularly to the large thin sections from the pit samples as it allowed a complete picture of the alpha particle distribution over the entire profile depth to be obtained. This enabled a) comparison to be made between measured analytical values for uranium and thorium and b) recognition of the overall spatial distribution of natural alpha particle activity in the soils and silts.

Preliminary modal assessment of this distribution was also made on a basis of counting of track densities. Exposure times for the autoradiographs were varied from one to six weeks, depending on the anticipated activity of the specimens, longest periods being given to the profile samples. After exposure, the plastic was etched in 6 molar NaOH solution to reveal the tracks.

The technique of autoradiography of natural alpha particle activity does not allow ready discrimination among the alpha-emitting nuclides of the uranium and thorium series, however, and the precise location of all uranium sites was achieved by recording fission fragments derived from uranium under neutron irradiation in a reactor [(n,f)reaction]. Interference from thorium was avoided by selecting a highly thermalised neutron flux in which only 235U undergoes appreciable fission. Irradiations were carried out at the Scottish Universities Research and Reactor Centre, East Kilbride. The method employed was based on that of Kleeman and Lovering (1967). "Lexan" polycarbonate plastic was used as a detector and tracks of the induced fission fragments revealed by etching for 5 minutes at 60^0C in 6 molar NaOH solution. The technique yields accurate spatial information on the location of uranium in the sample in the form of micromaps. Quantitative estimation of the uranium content of different host minerals was achieved by the irradiation of uranium-doped standard glasses along with the sample batches and consequent track counting on an equal area basis using an optical microscope. Neutron fluence was chosen to yield discrete tracks with minimum overlap to ensure reasonable counting accuracy (typically $2x10^{15}$ t.n.cm^{-2} is used). In some cases it was found necessary to make more that one fission track registration "print" at different neutron fluences in order to obtain workable track densities or to increase

sensitivity. In this way, uranium contents in the range 1 to several 100s ppm were measured with good reproducibility. Fission track study was made of all rock and vein samples together with, as indicated in Section 3.1, critical areas from the soil profiles which were selected on the basis of the initial autoradiographic examination.

3.3 SCANNING ELECTRON MICROSCOPY

Scanning electron microscope (SEM) analysis was carried out using a Cambridge Instruments Stereoscan S250 scanning electron microscope fitted with a 4-element solid-state (diode) backscattered electron detector (KE Developments Ltd). Mineralogical and chemical characterisation of phases imaged under the SEM was facilitated by qualitative observation of their energy-dispersive X-ray spectra. These were recorded using a Link Systems 860 energy-dispersive X-ray microanalyser (EDXA). The EDXA system has a detection limit of approximately 0.2 % (weight) for most common elements but this is probably of the order of 0.5% (weight) for U, Th and other heavy elements at typical count-times of 100 seconds and a beam potential of 20kV.

Analyses were largely carried out by backscattered SEM (BSEM) using polished thin sections. Routine secondary electron imaging techniques were also used to study rough stub-mounted rock fragments and plant roots in order to discern certain aspects of the characteristics of secondary uranium precipitation. The theoretical aspects of SEM techniques and their interpretation are discussed in detail by Goldstein *et al,* (1981) and the salient points are outlined below. Routine secondary electron SEM provides morphological information by imaging the low-energy secondary electrons produced in the specimen surface by interaction between the primary electron beam and the sample. The image brightness or shadowing depends largely upon the orientation of the surfaces being examined in relation to the electron beam and the electron detector. Polished thin-sections were studied in BSEM mode in which the images are related to the composition of the material being examined. Image brightness is proportional to the average atomic number of the material, thus allowing the distribution of different minerals or phases to be determined on the basis of their chemical composition. BSEM images are to some extent, affected by topography and are therefore normally used with flat or polished specimens. The technique can nevertheless be extremely useful in the location of dense trace minerals (which show up as bright grains) even in rough surfaces. BSEM has been used very effectively in the study of sediment diagenesis, mineralization and alteration (eg Krinsley *et al*, 1983; Huggett, 1984; Pye and Krinsley, 1984; Strong and Milodowski, 1987).

Rough surface, stub-mounted specimens were prepared by mounting pieces of rock, mineral or plant material onto aluminium pin-type SEM stubs using Leit-C conducting carbon cement. Plant material was initially prepared by freeze-drying and this was carried out using an Edwards Modulyo freeze-drier after rapid pre-freezing of the sample in liquid nitrogen. Prior to examination in the SEM the sections and stub-mounted specimens were coated with a thin film of carbon (approximately 200Å) by evaporation onto the specimen surface under vacuum. Most analyses were carried out at a 20kV beam potential.

In order to identify systematically the phases containing uranium, comparison was made of the SEM images from polished sections with fission track prints (Section 3.2) prepared from the same sections. Enlargements of the fission track prints were made by microfiche xerox-copier in order to produce a large-scale "map" of the uranium distribution for each polished section. From these maps it was possible to locate the uranium-bearing phases accurately and rapidly under BSEM in order to identify them by EDXA and determine their petrogenetic relationships. Identification of the uranium minerals was based on comparison of morphology and qualitative/semi-quantitative EDXA spectra with published data (eg Palache *et al*, 1951; Durrance, 1986)

4. SOURCE ROCK MINERALIZATION AND LOCATION OF URANIUM

4.1 GENERAL

The principal features of the analogue site are described in Roberts *et al*, (1988) and a geological map, revised from that of Miller and Taylor (1966) as a result of recent detailed fieldwork, is shown in Figure 2. Two major breccia veins are exposed in the cliff face, and these unite towards the top of the cliff and continue northwards under a cover of till towards the granodiorite. The lithologies at the site are highly fractured and five generations of faulting and shearing are discernible. The felsite dykes were emplaced very early on in the structural sequence indicating their temporal association with the granodiorite. Both these lithologies were subsequently affected by several episodes of faulting and fracturing including coastal shearing, before the northwest-trending mineralized veins were emplaced. The metalliferous veins are restricted to within the hornfelsed aureole and tend to be concentrated in fractures at the margins of felsite bodies. Thus they appear to be related to fluids migrating through a brittle zone surrounding the granodiorite intrusion where open fractures would preferentially develop within the hornfelsed sediments.

Trenching of both parts of the structure was carried out by Miller and Taylor (1966) and access to mineralized vein material was obtained from these old workings. Beneath the cliff face, radiometric anomalies were established by the early survey to relate to extension of the mineralization seaward below the coastal sediments to beyond the main coastal fault. The present study of the site as a natural analogue considers the uranium-bearing vein as the "source-term" with dissolved radioelements being transported by surface waters and by the groundwaters percolating through fissures in the highly-fractured rocks of the cliff and retarded by the coastal silts and overlying peaty soils.

A preliminary re-appraisal of the mineralization as the uranium source-term for the natural analogue study, was reported by Basham and Hyslop (1989). The vein mineralogy within the site is in keeping with the notably consistent regional style, being polymetallic in uranium, copper, bismuth, cobalt and nickel (with arsenic, antimony). Samples collected across the trenched vein towards the top of the cliff (Locality V, Figure 2), show the characteristic assemblage of uraninite (var. pitchblende), hydrocarbon, pyrite, chalcopyrite and bismuth in quartz-calcite-dolomite-gangue. Minor amounts of other ore minerals include digenite, galena and finely disseminated nickel-arsenic phases. Where sampled, the vein occupies a brecciated fracture system, about 0.7m wide, along the near-vertical contact between a tongue of porphyritic granodiorite and hornfelsed siltstone (Plate 3). The country rock in particular is highly fractured and mineralized in both uranium and sulphides, oxidation of the latter imparting a distinct yellow-brown or occasionally green (secondary copper minerals) colouration. Fracturing in the hornfels has resulted in the development of a regular system of close-spaced minor joints along which the rock has a tendency to break up into regular blocks.

4.2 VEIN MINERALIZATION

4.2.1 Granodiorite Wallrock

4.2.1.1 *Mineralogical Assemblage*

The granodiorite comprising the wallrock of the carbonate-sulphide-uraninite vein mineralization contains evidence of a complex history of mineralization and alteration and some of these features are common to the local granodiorite more distant from the veins. The earliest mineralization event involved the formation of fine veinlets (10-100μm) of K-feldspar and quartz or K-feldspar alone. BSEM shows that the feldspar occasionally displays rhombic "adularia" habit characteristic of hydrothermal K-feldspar. These veinlets

are cross-cut by quartz veinlets made up of anhedral, decussate quartz. A possible second generation of fine veinlets of K-feldspar may cut the quartz veinlets but the relationship is unclear and requires further examination. BSEM study suggests that larger scale potassic alteration of the granodiorite matrix may possibly be associated with the K-feldspar-bearing veinlets, manifesting itself in the apparent replacement of primary plagioclase by K-feldspar. Again, the precise character of the K-feldspar is unclear and requires more detailed appraisal.

Apparent K-feldspar replacement of the granodiorite has resulted in corroded relicts of plagioclase (unlike exsolution intergrowths) within large patches of K-feldspar. Associated in these patches are inclusion trails (unrelated to the present crystallography of the host phase) of zircon and a thorium-uranium silicate with tetragonal morphology (probably thorite; $ThSiO_4$ or uranothorite; $(Th,U)SiO_4$). These inclusions appear to delineate the boundaries of replaced grains, in "ghost fashion" (Plate 4) or have grown along grain boundary cracks (Plate 5). Detailed BSEM examination reveals that the zircon and thorite/uranothorite are closely associated and often intergrown, although the common interstitial relationship of the latter suggests slightly later growth (Plate 6).

Much reddening of feldspars and alteration of micas is related mainly to small fracture veinlets filled with carbonate which comprises either calcite alone (Plate 4) or a complex of relict dolomite largely replaced by calcite (Plate 7), carrying sulphides (mainly chalcopyrite). Fine hematite is dispersed along the cleavages of the calcite (Plate 7) and altered feldspar. Some fine veinlets (c. 1mm) consist almost entirely of chalcopyrite either enclosing minor pyrite or with pyrite at the vein walls. Most of these veinlets show oxidative alteration along their margins to fine grained iron oxides, pyrite seemingly to have been preferentially oxidised (Plate 8). Fine grained secondary chlorine-bearing copper minerals and rare nickel silicate coatings are associated with this oxidation. The character of the copper secondaries is consistent with earlier reports (Miller and Taylor, 1966) of atacamite ($Cu_2Cl(OH)_3$) or connelite ($Cu_{19}Cl_4(OH)_{32}.H_2O$) but precise identifications have not been made. The carbonate-sulphide veinlets cross-cut the earlier adularia (±quartz) and quartz veinlets. In some cases the carbonate veinlets exploit earlier adularia veinlets, and relict partly replaced adularia crystals can occasionally be found in the carbonate.

4.2.1.2 *Uranium Locations*

Within the granodiorite matrix, uranium sources giving rise to discrete fission track clusters can be equated by BSEM-EDXA to zircons, thorite/uranothorites, a thorium-silicon-phosphorus mineral (possibly a phosphatic variety of thorite or huttonite), monazite

((Ce,La,Nd,Th,U,Ca)PO_4), xenotime (YPO_4) and apatite ($Ca_5(PO_4)_3OH$). These minerals occur in crystals 1-10μm in size, the most abundant being thorite/uranothorite, zircon and apatite, in order of relative uranium content. The other minerals are relatively rare. A number of these grains display alteration (possibly associated with some degree of metamictisation) or complex intergrowths of various phases. Some thorite/uranothorite grains are possibly intergrown with monazite and altered to a rhabdophanic or thorogummite-like mineral.

Thorian monazites occasionally display alteration along microcracks (Plate 9) to less-dense low-thorium monazite or rhabdophane ((Ce, La, Nd)$PO_4.nH_2O$). Lanthanum appears to be depleted relative to cerium in the secondary product. Uranium is detectable in xenotime but occasionally discrete uranium silicate inclusions are evident from BSEM-EDXA observations.

Within the areas of carbonate-sulphide alteration and veining uranium is located by fission track study with fine-grained, opaque material, shown by SEM to comprise mixtures of sulphides (mainly chalcopyrite) and iron oxides. The oxidised vein margins (Plate 8) can contain uranium in levels up to 1%, possibly indicating absorption from supergene waters. Uranium is also detectable by EDXA in some areas of secondary iron oxide associated with significant concentrations of arsenic, copper and zinc and discrete grains (1-5μm) of a uranium-silicate mineral are seen occasionally. The finely divided nature of these sites implies high surface areas with potential as available sites for release or sorbtion of analogue elements.

4.2.2 Main Carbonate Vein

4.2.2.1 *Mineralogical Assemblage*

Results from this study, particularly with the use of BSEM-EDXA, show that the vein assemblage is more complex and varied than previously described by Miller and Taylor (1966). In the field, the vein is strongly banded parallel to its strike. Two prominent zones of mineralization can be seen and in thin section the banding is seen to be the result of shearing and brecciation of the earlier episode of mineralization. Much of the earlier event has been overprinted and replaced by subsequent carbonate mineralization and it appears that the veins re-opened during this second stage by failure along the contact with the brittle hornfels.

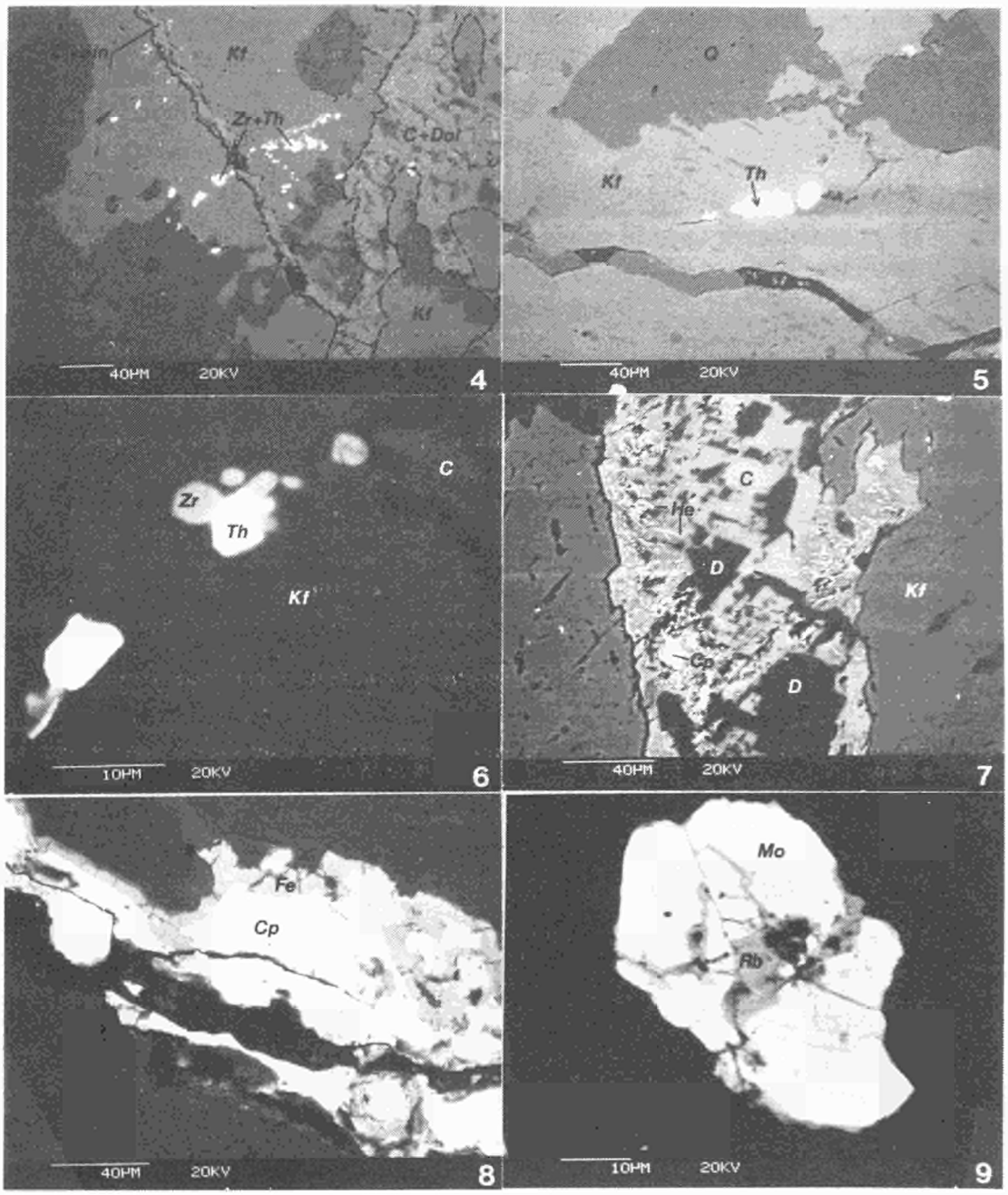

PLATE 4 BSEM photomicrograph of altered granodiorite wallrock showing veinlets of calcite (C) and dolomite (Dol) cutting across K-feldspar (Kf) and quartz (Q) of the granodiorite. Note ghost outlines of former grain boundaries, now overprinted by K-feldspar, picked out by zircon (Zr) and thorite (Th). Relict plagioclase present in K-feldspar.

PLATE 5 BSEM photomicrograph showing thorite (Th) crystallised along grain boundary cracks in K-feldspar (Kf). Quartz grains (Q) and fine quartz veinlet also seen.

PLATE 6 Detailed BSEM photomicrograph showing associated euhedral thorite (Th) and zircon (Zr). Note thorite partly interstitial to zircon crystals.

PLATE 7 BSEM photomicrograph showing complex carbonate veinlet with relicts of earlier dolomite (D) partly replaced by later calcite (C). Hematite (He) present along calcite cleavages adjacent to vein border. Veinlet seen cutting and partly replacing K-feldspar (Kf). Chalcopyrite (Cp) also present.

PLATE 8 BSEM photomicrograph showing oxidation of chalcopyrite (Cp) and veinlet edges with production of secondary ferric oxide (Fe).

PLATE 9 BSEM photomicrograph showing alteration of thorian monazite to low-Th monazite or rhabdophane (Rb) along microcracks.

The earliest mineralization consists of quartz and K-feldspar and occurs in the band adjacent to the granodiorite wallrock. Granular intergrowths of K-feldspar and quartz occur as relict patches or "pods" largely replaced and enclosed within later dolomite and calcite (Plate 10). The K-feldspar often displays rhomb-morphology of adularia (Plate 11) but much of the quartz-K-feldspar mineralization is sheared parallel to the vein walls (Plate 10) and minor sericite and chlorite developed. Tetragonal crystals of an yttrium phosphate mineral (probably xenotime; YPO_4) are abundant within the K-feldspar-quartz relicts (Plate 12). These are later than the quartz-K-feldspar mineralization and are particularly concentrated along the quartz grain boundaries within the relicts (Plate 13) or along the surfaces of dolomite rhombs at the margins of the relicts (Plate 12). Micaceous hematite is closely related to the alteration of the quartz-K-feldspar relicts and is sometimes seen, accompanied by fine secondary TiO_2, replacing associated muscovite. Hematite also often accompanies the secondary xenotime (Plate 14) but the xenotime appears to slightly post-date hematite as plates of the latter are often seen trapped within xenotime crystals.

The major minerals in the vein are dolomite and calcite with minor to accessory hematite, chalcopyrite, pyrite, digenite, galena, pitchblende and globular brittle hydrocarbon being the most obvious or common ore minerals. Dolomite appears to be the earliest of these phases (cf also Miller and Taylor, 1966) and is brecciated and replaced by the later calcite which occurs interstitially. The sulphide mineralization is dominated by chalcopyrite which commonly includes earlier precipitated pyrite and may be altered to or replaced by other sulphides including digenite, chalcocite (Cu_2S), bornite (Cu_5FeS_4) and galena (PbS). Minor sphalerite (ZnS) is common and is usually rimmed by overgrowth of chalcopyrite. The sulphide minerals post-date dolomite, occurring enclosed within the calcite but mineralizing the brecciated surfaces of the dolomite. Rarer bismuth sulphide and native bismuth or bismuth oxide accompany the more common sulphides.

Uraninite is also closely associated with the dolomite and possesses the characteristic botryoidal form of the low temperature variety pitchblende (Plate 21). The pitchblende is slightly later than dolomite and can be seen to coat dolomite rhombs (eg Plate 15). Individual grains range up to 5mm across and show typical syneresis cracks filled by later calcite with a secondary platy to fibrous uranium-arsenic mineral (Plate 16). The mode of occurrence, platy morphology and qualitative chemistry of this secondary mineral are consistent with troegerite; $(H_3O)_2(UO_2)(AsO_4)_2.H_2O$ (Palache *et al*, 1951). However, this identification has not been confirmed by quantitative analysis or X-ray diffraction techniques. Sulphides are occasionally present in the shrinkage cracks. Many pitchblende grains are corroded and etched (Plate 17). Clausthalite (PbSe), with similar appearance and cubic morphology to

galena, closely accompanies and may be intergrown with the pitchblende (Plate 17). Clausthalite has not previously been reported from this locality.

Globular hydrocarbon is a common component in the veins (Plates 23 and 25), infilling vuggy cavities in dolomite or in similar mode to pitchblende. The presence of unmineralised "gas bubble" cavities, typically 1-5μm diameter are commonly visible under SEM. Miller and Taylor (1966) described the hydrocarbon as replacing pitchblende but this relationship was not evident from the present sections. However, the occurrence of the hydrocarbon in sites similar to that of pitchblende may be indicative of hydrocarbon replacement of pitchblende. Vuggy cavities in dolomite, up to 5mm across may be lined by smokey quartz and platy hematite (cf also Miller and Taylor, 1966). Smokey quartz is often taken to indicate the presence of uranium mineralization (Heinrich, 1958).

Cracks in the calcite and dolomite gangue are coated with fine secondary iron-manganese oxides, copper-chlorine minerals and numerous secondary minerals containing copper, arsenic, iron, nickel and cobalt.

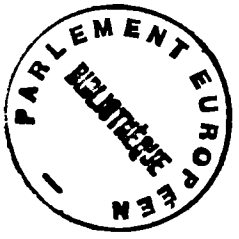

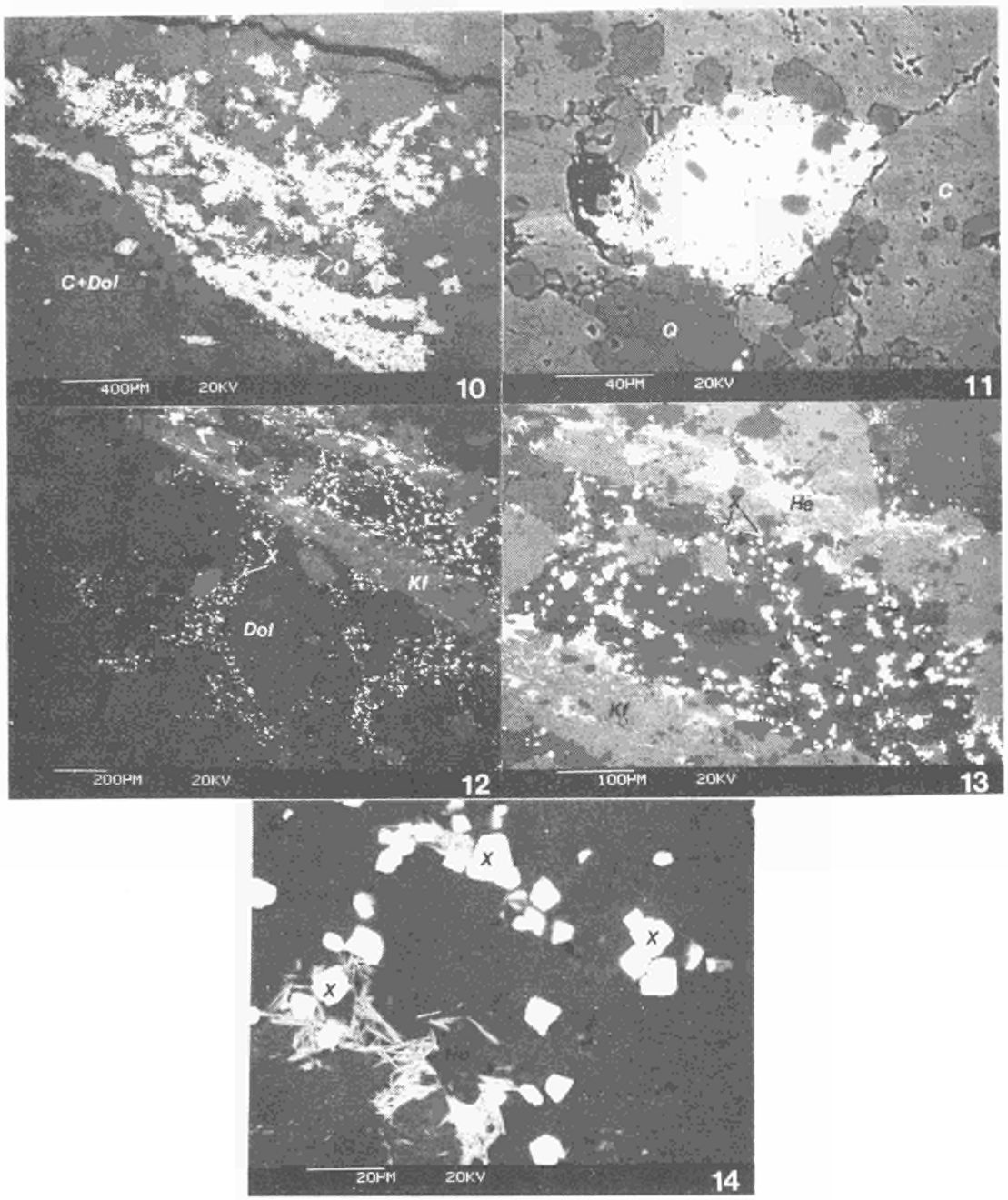

PLATE 10 BSEM photomicrograph showing relict of earlier intergrown quartz (Q) and K-feldspar (Kf) mineralization largely replaced by later calcite (C) and dolomite (duller, Dol) mineralization. Tiny bright secondary xenotime crystals are associated with the surfaces of the relict earlier mineralization.

PLATE 11 BSEM photomicrograph of relict early K-feldspar-quartz mineralization showing adularia-like crystals (Ad) of K-feldspar intergrown with quartz (Q) largely overprinted by later replacive calcite (C).

PLATE 12 BSEM photomicrograph showing abundant bright xenotime crystals (X) precipitated around dolomite (Dol) rhombs and strongly associated with relict early K-feldspar- quartz mineralization (Kf).

PLATE 13 BSEM photomicrograph showing concentration of xenotime (X) along quartz (Q) grain boundaries in relicts of quartz-K-feldspar mineralization. Bright micaceous hematite (He) also present.

PLATE 14 BSEM photomicrograph showing tetragonal crystals of xenotime (X) associated with micaceous hematite (He) in matrix of granular quartz. From relict early K-feldspar-quartz mineralization.

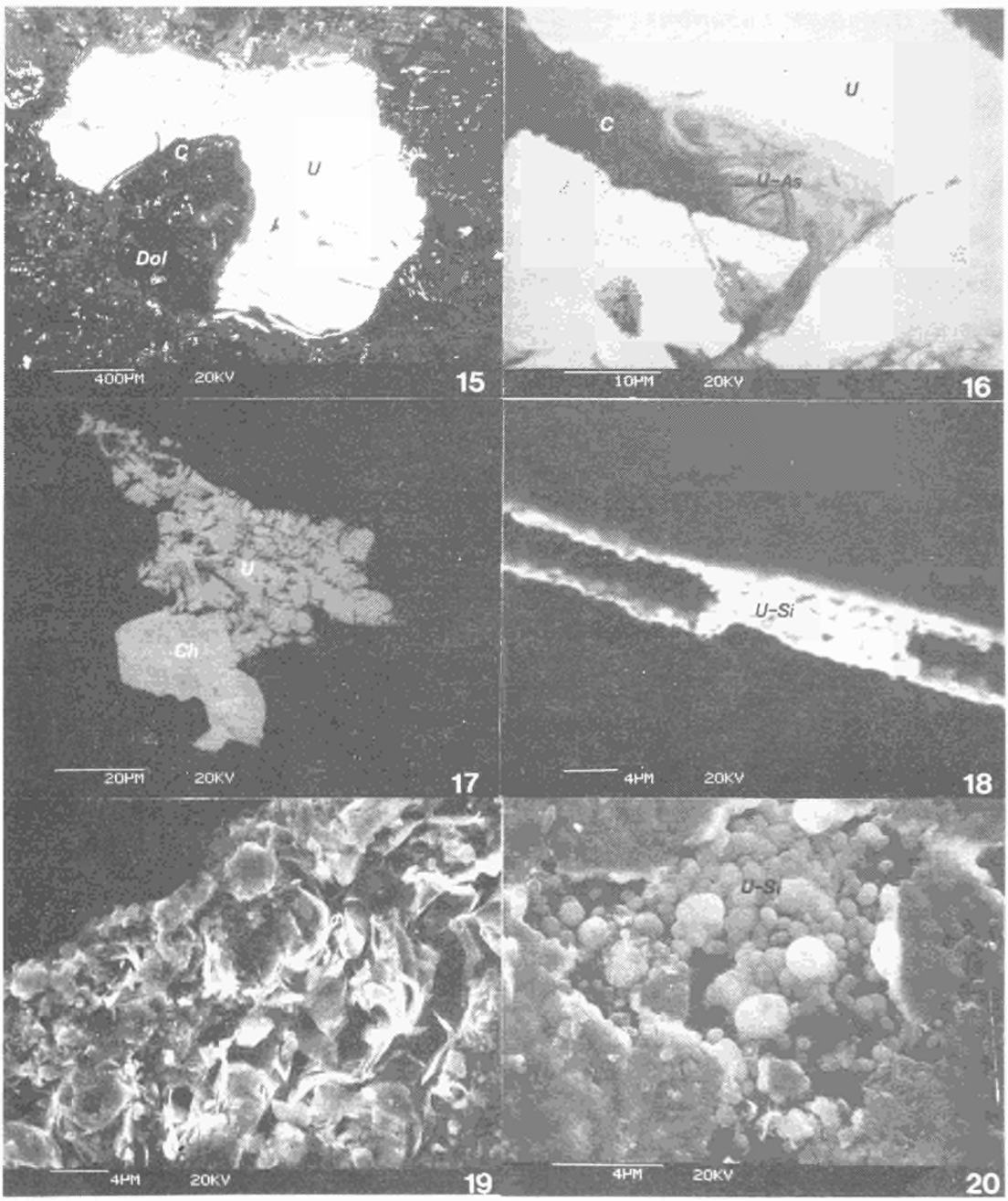

PLATE 15 BSEM photomicrograph showing a large bright uraninite (U) grain (variety pitchblende, cf also Plate 21) growing replacively around a brecciated dolomite rhomb (Dol). Finer bright uraninite and sulphides can also be seen along brecciated dolomite surfaces. Later calcite (C) is seen as a mid-grey phase replacing dolomite along brecciated surfaces and cleavage planes. Uraninite displays syneresis cracks.

PLATE 16 BSEM photomicrograph of platey to fibrous uranium-arsenic mineral (U-As), possibly troegerite, associated with calcite (C) infilling syneresis cracks in uraninite (U).

PLATE 17 BSEM photomicrograph showing etched and corroded uraninite grain (U) associated with cubic morphology clausthalite (Ch) in calcite gangue.

PLATE 18 BSEM photomicrograph of fracture in brittle vein hydrocarbon (in situ) infilled by very fine grained uranium silicate mineral (U-Si) which can be seen slightly replacing the hydrocarbon of the fracture wall.

PLATE 19 SEM photomicrograph of fracture in brittle vein hydrocarbon from a loose block mineralized by platey morphology uranium-arsenic mineral, possibly troegerite.

PLATE 20 SEM photomicrograph of microspheroidal uranium silicate phase coating the surface of a globule of brittle vein hydrocarbon in contact with carbonate gangue.

4.2.2.2 *Uranium Locations*

Autoradiographic and fission track studies show that the principal host for uranium in the carbonate vein is the pitchblende (Plates 21 and 22). As to be expected from the genesis and form, the content of thorium is too low to be detected by EDXA, in keeping with the chemical analysis given for a concentrate from the nearby Steps Vein used for age determination (185 ±20my) in Miller and Taylor (1966). As such, solubility in oxidising waters is potentially high, a conclusion supported by the observation of decomposed pitchblende and high dispersed radioactivity in the dumps from Miller and Taylor's trenching of the vein.

Parnell (1988) and Eakin (1989) report contents of 4.5% and 35.89% by weight uranium respectively in hydrocarbons from this locality. Inclusions of pitchblende, referred to by Miller and Taylor (1966) and Parnell (1988), were not seen in the present study and do not appear to make a significant contribution to the mass balance. Track registration techniques show that the hydrocarbon mass itself contains negligible intrinsic uranium but fission track distributions indicate a close association of significant levels of uranium with grain surfaces or internal cracks (Plates 23 and 24). BSEM observation of these fractures and grain surfaces identified very fine grained uranium (±bismuth)-silicate as coatings and replacements of the immediately underlying hydrocarbon substrate (Plate 18). The uranium silicate possesses no morphological characteristics to aid precise identification but possible identifications would be coffinite ($U(SiO_4)_{1-x}(OH)_{4x}$) or soddyite ($(UO_2)_5Si_2O_9.6H_2O$). The cracks in the hydrocarbon are later than those in the pitchblende and do not appear to be infilled by calcite.

SEM examination of open fracture surfaces of hydrocarbon collected from exposed outcrop and loose blocks from the earlier trenching revealed a much more complex association of uranium. Many fracture surfaces have a greenish-yellow coating consisting of fine platelets of a uranium-arsenic mineral which may be troegerite (Plate 19). Surfaces in contact with the carbonate matrix may also be coated with fine grained uranium-calcium-arsenic (?uranospinite; $Ca(UO_2)_2(AsO_4)_2.10H_2O$) and possibly rare uranium-magnesium-arsenic (?novacekite; $Mg(UO_2)_2(AsO_4)_2.12H_2O$) minerals, in addition to microspheroidal uranium-silicate (Plate 20). Parnell (1988) also suggests that troegerite and zeunerite ($Cu(UO_2)_2(AsO_4)_2.10\text{-}16H_2O$) occur as fracture coatings in the hydrocarbon globules from Needle's Eye. Several fracture surfaces in hydrocarbon reveal the presence of peculiar uraniferous filaments apparently of organic origin (Plate 27). These filaments form loops and may "bridge" one another (Plate 28). They display dendritic "fruiting bodies" (Plate 29) and fine branching porous "microfilaments" or "hyphae" penetrate from the main filaments

into the surrounding hydrocarbon (Plate 30). These features are present only on fracture surfaces and not in the bulk of the hydrocarbon. Often a mineralized tangled mass of filaments coats the hydrocarbon surface adjacent to the main filaments (Plate 31). Under high magnification the filaments display evidence of a cellular structure (Plate 32). The associated mineralization is very complex. The central core of the main filaments and cells is mineralized with a dense bismuth-sulphur phase containing minor amounts of copper, nickel, zinc, arsenic and selenium and may correspond to bismuthinite (Bi_2S_3) or some other bismuth-sulphosalt. The walls of the cells and filaments are mineralized by uranium and calcium (possibly an oxide eg becquerelite; $CaU_6O_{19}.11H_2O$ or a carbonate eg liebigite; $Ca_2(UO_2)(CO_3)_3.10H_2O$) and in some cases by possible native selenium. The fine filaments and amorphous "mucilage" around the main filaments are enriched in uranium, calcium and vanadium whilst aggregated fine plates of a calcium-uranium-rich mineral appears to nucleate within the fine filaments-mucilage mass (Plate 33). Although the tabular morphology resembles that of liebigite (Palache *et al*, 1951), a number of other uranium minerals commonly occur in similar form and positive identification would require X-ray photography.

Fission track prints also show the common occurrence of fine disseminations of uranium along grain surfaces of pyrite, chalcopyrite, digenite and galena (Plates 25 and 26). This association is considered to be quantitatively more important than the hydrocarbon association, in view of the frequency of the sulphides and the tendency of most to become altered within the weathering zone. BSEM shows that the main phase hosting uranium in this association is a uranium-silicate (possibly coffinite or soddyite but no distinctive morphology is shown to aid identification). The uranium-silicate is fine grained and nucleates largely upon chalcopyrite surfaces, replacing the underlying sulphide substrate (Plate 34) where it may also accompany galena and bismuth-sulphide replacement of chalcopyrite. Fission tracks concentrated around other sulphides (pyrite, sphalerite) are similarly associated with uranium-silicate, invariably replacing chalcopyrite overgrowths.

In addition to enrichments associated with surface-active amorphous iron oxide weathering products, minor secondary uranium-arsenic-lead-silicate phases occur replacing dolomite. It would appear that hydrated uranium silicate minerals (eg boltwoodite; $(H_3O)K(UO_2)(SiO_4).H_2O$) are the most common secondary minerals regionally but the copper-uranium arsenide zeunerite is also common (Miller and Taylor, 1966; Parnell, 1988). In the present study, boltwoodite has not been encountered and another uranium-silicate (possibly coffinite or soddyite) is by far the most abundant uranium mineral (other than pitchblende) found in the carbonate vein. Locally, unusual species such as vandendreisserite (uranium-lead oxide), have been recorded by Miller and Taylor (1966) but have not yet been

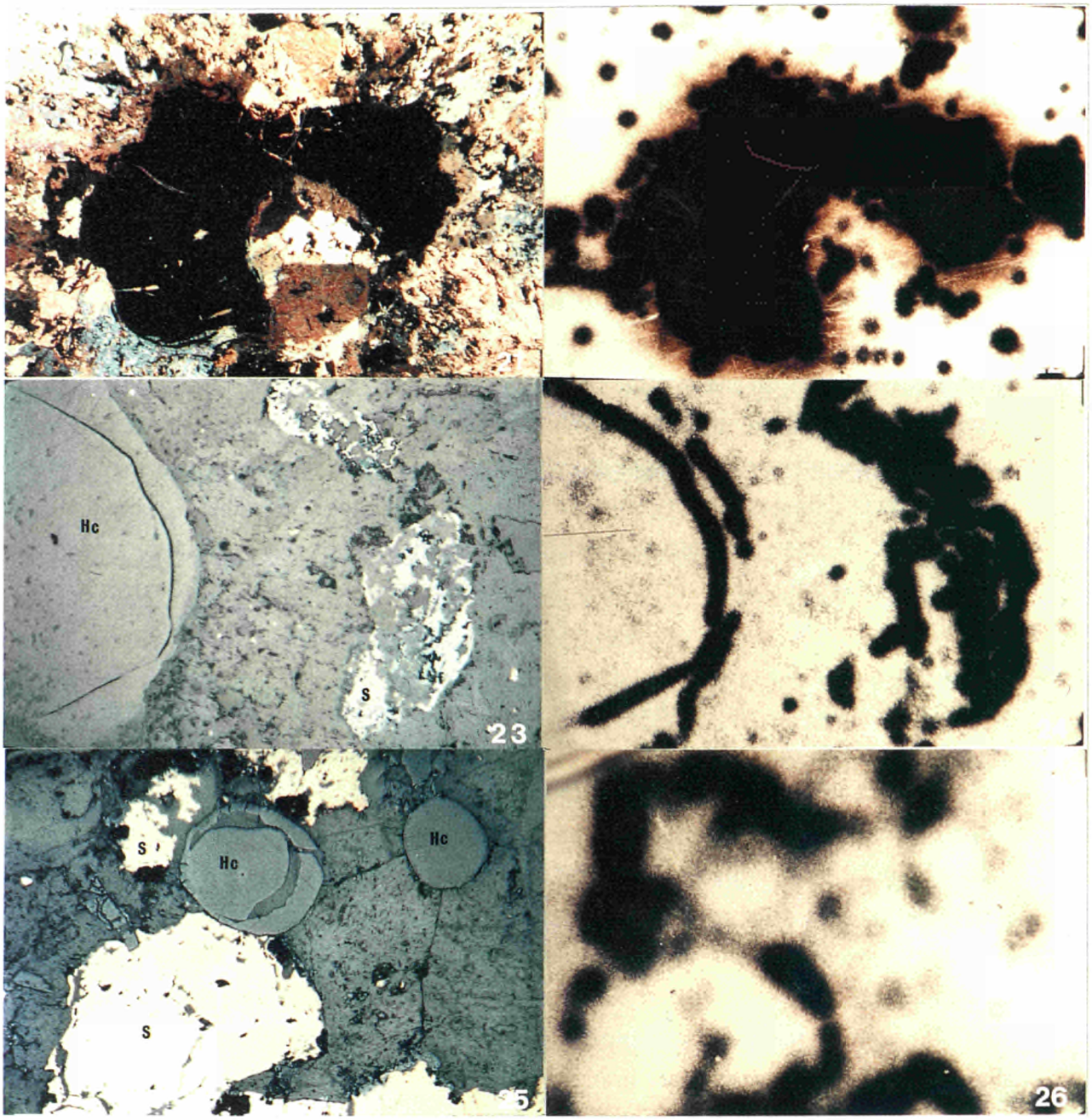

PLATE 21 Botryoidal pitchblende in carbonate gangue (cross polarised transmitted light). Note syneresis cracks penetrated by carbonate and possibly other uranium bearing minerals. Field width: 10mm.

PLATE 22 Fission track print of Plate 21 showing concentration of uranium within pitchblende, on surfaces and in associated minerals in the carbonate gangue.

PLATE 23 Globular hydrocarbon (Hc) and sulphides (S), mainly digenite, in carbonate gangue. Reflected light. Field width: 5mm.

PLATE 24 Fission track print of Plate 23 showing association of uranium with surfaces and cracks within the hydrocarbon, and on sulphide grain surfaces. Note very low track density within the hydrocarbon and in the carbonate gangue.

PLATE 25 Globular hydrocarbon (Hc) and sulphides (S), pyrite and chalcopyrite, in carbonate gangue. Reflected light. Field width: 5mm.

PLATE 26 Fission track print of Plate 25 showing association of uranium with sulphide grain surfaces.

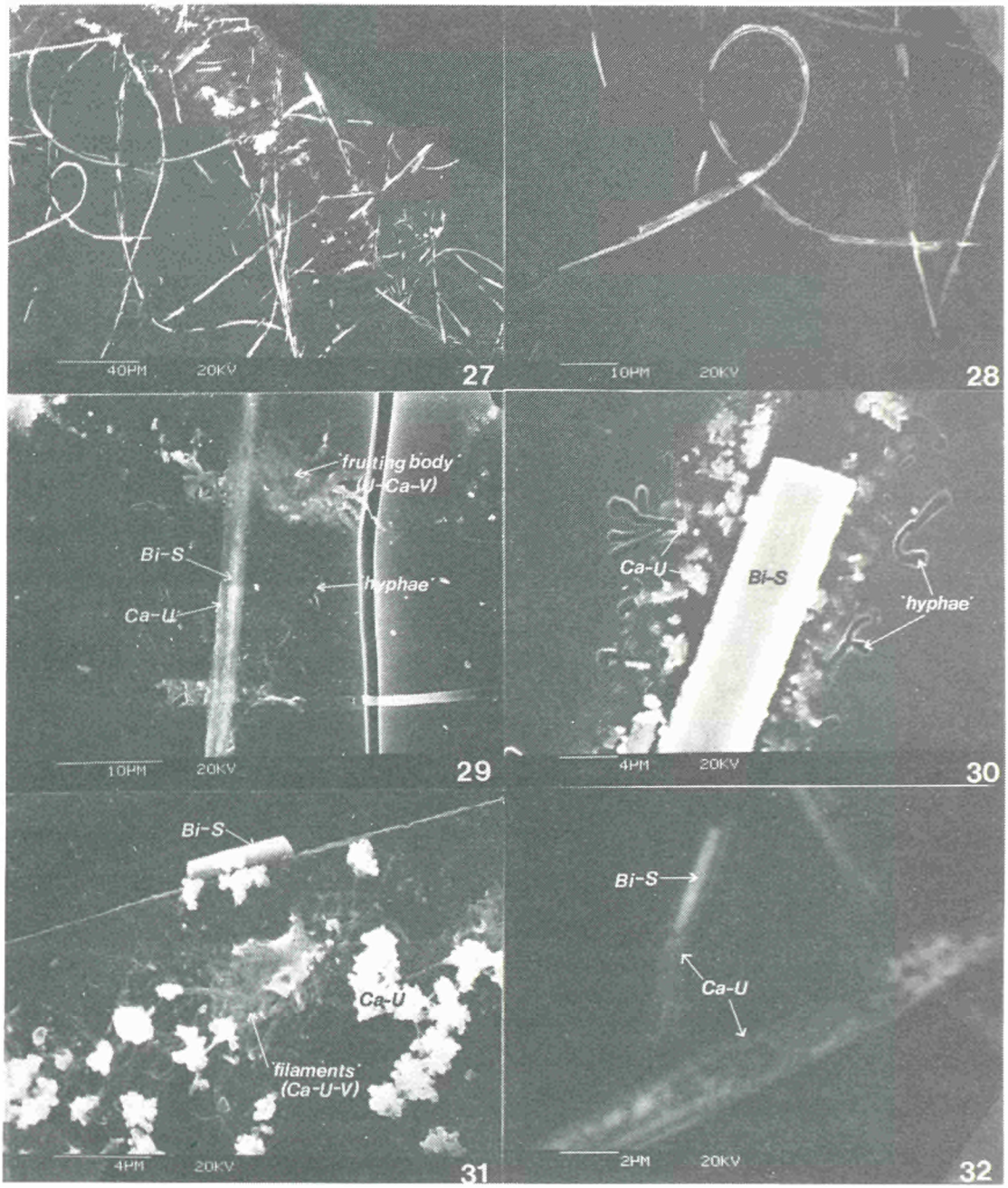

PLATE 27 BSEM photomicrograph of open fracture surface (unpolished) in brittle vein hydrocarbon globule showing presence of bright uraniferous organic filaments. Note loop features.

PLATE 28 Detail of Plate 27 showing loop feature and bridging filaments.

PLATE 29 SEM photomicrograph showing fine structure of the uraniferous organic filaments: core of main filament mineralized by bismuth sulphide (Bi-S); walls of main filament mineralized by a calcium uranium phase (Ca-U); dendtritic "fruiting body" mineralized by an uranium-calcium-vanadium phase (U-Ca-V). Unmineralized fine filamentous side-branching structures ("hyphae") "eat" into the hydrocarbon adjacent to the main filaments.

PLATE 30 Detailed BSEM photomicrograph of filaments showing dense bismuth sulphide mineralized core (Bi-S), fine platey calcium-uranium mineral (Ca-U) along borders of filament and unmineralized side branching "hyphae" eating into the hydrocarbon.

PLATE 31 BSEM photomicrograph of fracture surface in hydrocarbon showing fine mucilage of calcium-uranium-vanadium mineralized filaments (Ca-U-V) adjacent to largely bismuth sulphide mineralized main filament (Bi-S). Platey calcium-uranium mineral (Ca-U) can be seen nucleating amongst the fine filamentous mucilage.

PLATE 32 BSEM photomicrograph of the main filaments showing cellular structure: centre of cells are mineralized by bismuth sulphide (Bi-S); cell walls are enriched in calcium and uranium (Ca-U).

found in this study. In view of the complexity of the polymetallic mineralization and the large number of possible chemical combinations in which uranium minerals can occur, it is highly likely that extended detailed BSEM study would reveal further secondary uranium minerals in these veins.

4.2.3 Hornfels Wallrock

4.2.3.1 *Mineralogical Assemblage*

The hornfels wallrock is a siltstone composed of a deccussate granular mosaic of major quartz, K-feldspar, plagioclase and biotite. Grain size is typically 20-40μm, i.e. coarse siltstone. Biotite flakes show a strong preferential alignment parallel to the foliation and similarly, quartz and feldspar grains show growth elongation parallel to this direction. This results in some degree of fissility and a tendency to fracture along the oriented fabric, accounting for the extremely brittle and intensely fractured nature of the hornfels. Many of the fine mineralized veinlets described below exploit this inherent weakness in the rock.

The features of the vein mineralization are generally similar to those seen in the granodiorite wallrock, the earliest veins being fine (20-60μm wide) veinlets of K-feldspar (adularia) approximately normal to the foliation (Plate 35). As in the granodiorite, these veinlets are cross-cut by later granular anhedral quartz veins. These in turn show some possible evidence of being cut by a second but less well-developed generation of adularia veinlets but, again as in the case of the granodiorite, the precise relationship of these later veinlets is not clear. Minor wallrock alteration occurs around these veinlets, marked by very minor wallrock replacement by K-feldspar adjacent to adularia veins and the development of coarser biotite adjacent to the quartz structures. Some biotite occurs within the quartz veins, and both this and the adjacent wallrock biotite may display minor hematisation. A later generation of fine chlorite-filled veinlets cuts across the earlier mineralization described above. These veins are open and the (iron-rich) chlorite has partly altered to iron oxides (Plate 36). The presence of minor calcium in the chlorite may be indicative of some component of smectite mixed-layering. The latest veinlets are composed of dolomite and calcite, as in the granodiorite wallrock.

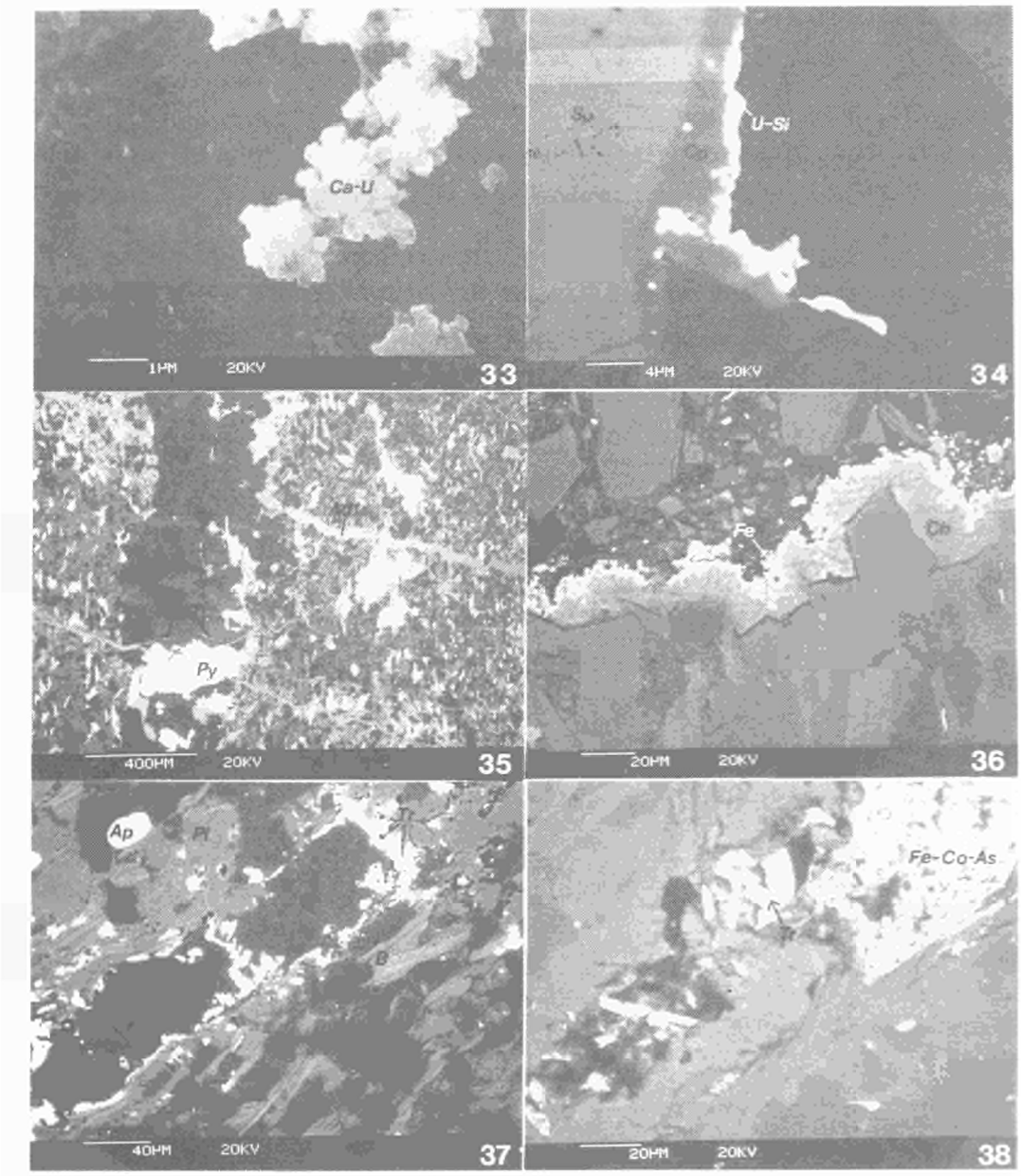

PLATE 33 SEM photomicrograph showing detail of platey morphology of calcium-uranium mineral associated with mucilage around uraniferous organic filaments on fracture surface of brittle hydrocarbon globule.

PLATE 34 BSEM photomicrograph of complex sulphide mineralization in main carbonate vein showing overgrowth of sphalerite (Sp) by slightly later chalcopyrite (Cp). Note replacement of chalcopyrite by bright uranium silicate (U-Si) at surface of sulphide.

PLATE 35 BSEM photomicrograph of quartz veinlet (Q) in hornfels. The veinlet is parallel to the foliation of the rock picked out by the micaceous minerals (largely biotite, mid to light grey). Early adularia veinlets (Ad^1), cutting the foliation, are cut by the later quartz veinlet. A possibly later but weakly-developed generation of adularia veinlets (Ad^2) cut the quartz veinlet. Minor sulphide mineralization, mainly pyrite (Py) is associated with the quartz.

PLATE 36 BSEM photomicrograph of chlorite (Ch) veinlet cutting foliation of hornfels and altered on its exposed surface to iron oxides (Fe).

PLATE 37 BSEM photomicrograph of quartz-filled veinlet in hornfels showing platey uranium-arsenic mineral, probably troegerite (Tr) encrusting quartz surfaces. Apatite (Ap), plagioclase (Pl), K-feldspar (Kf) and biotite (B) of the hornfels also indicated

PLATE 38 BSEM photomicrograph of cavities associated with quartz veinlets, infilled by possible troegerite (Tr) and iron-cobalt-arsenate (Fe-Co-As).

Sulphides are associated with both the quartz and carbonate veinlets. In the quartz veins the pyrite is the major sulphide but chalcopyrite is dominant in the carbonate veins. Minor galena, copper-sulphide (possibly digenite or covellite), bismuth-sulphide, arsenic-iron-copper-bismuth-sulphide and copper-antimony-arsenic-iron-zinc-sulphide are also present. Rare grains of acicular native bismuth , native silver and native gold accompany the sulphides. Oxidative alteration of the sulphide minerals is apparent in most veinlets with the production of secondary goethite along vein margins and minor baryte is sometimes present in the secondary oxide. Some sulphide-bearing veinlets contain iron-nickel-cobalt-arsenate secondary alteration products.

4.2.3.2 *Uranium Locations*

The principal association of uranium in the veinlets is shown by fission track study to be with secondary iron oxide alteration products of sulphides (Plates 39 and 40). No discrete uranium phases are present in this association which probably results from supergene sorbtion onto the secondary iron oxide. Dense fission track lineations were also correlated by BSEM with the oxidised chlorite in "open" veinlets. Very dense, discrete clusters of fission tracks within some quartz or adularia veinlets (Plates 41 and 42) were found to correspond to sheaf-like clusters of platy or micaceous greenish-yellow crystals which were identified by EDXA as a uranium-arsenic mineral. The colour, habit and major element chemistry suggest this phase to be troegerite. It occurs encrusting the quartz grains (Plate 37) or as coarser crystals in cavities in the veins where it is closely associated with a fine grained iron-cobalt-arsenate (Plate 38). Uraniferous veinlets of this type extend to around 1m from the main vein and secondary uranium minerals can be detected radiometrically over a distance of several metres at least.

Within the hornfels matrix a number of discrete fission track clusters can be related to detrital zircons and thorium-bearing monazite. Although uranium was not detectable by EDXA within these minerals it is nevertheless most likely present at relatively high concentrations (several hundreds ppm).

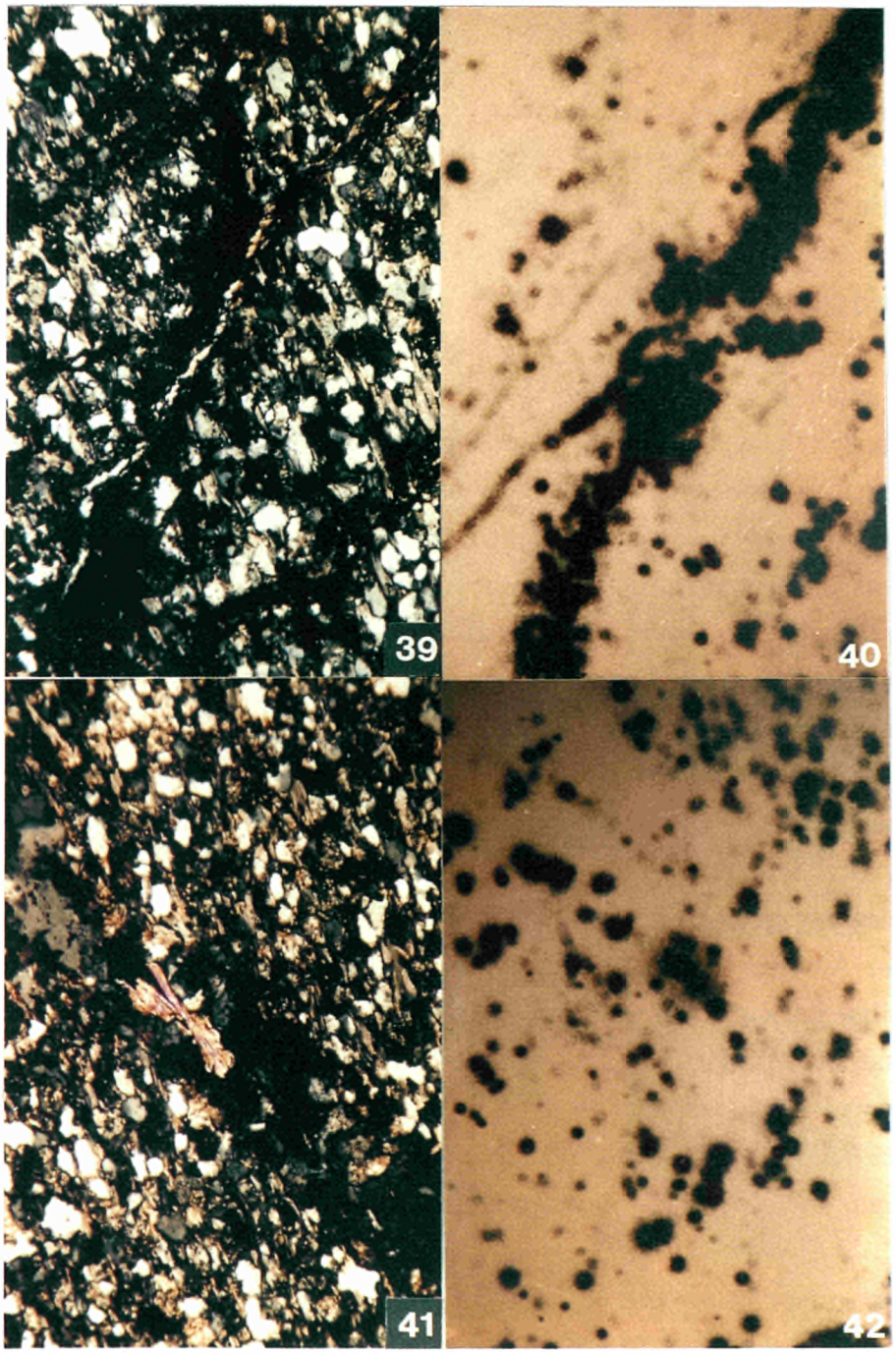

PLATE 39 Siltstone wallrock (cross polarised transmitted light) with fine fracture veins containing fine secondary iron oxidation products of sulphides. Field width: 5mm).

PLATE 40 Fission track print of Plate 39.

PLATE 41 Siltstone wallrock (cross-polarised transmitted light) with cross-cutting quartz-adularia vein containing a sheaf-like cluster of a platey secondary uranium mineral. Field width: 5mm.

PLATE 42 Fission track print of Plate 41. A large halo of tracks corresponds with the uranium mineral, in contrast to the numerous discrete spots associated with detrital minerals in the siltstone or sites of uranium adsorption.

4.3 GRANODIORITE

The presence of leachable uranium minerals in the marginal phases of the pluton within and above the cliff at the analogue site would have important implications in the modelling of dispersion in groundwaters. No systematic sampling has been carried out at present but a preliminary study of samples from elsewhere in the "background" granodiorite has demonstrated their potential for inclusion as "source-terms".

Accessory uranium-bearing minerals so far recognised include common zircon, sphene, and apatite with, less frequently, allanite, thorite and uraninite. By analogy with other plutons in the province, additional minerals such as monazite and xenotime are also likely to occur in parts of the fractionation sequence. Zircon, sphene and apatite are usually relatively stable minerals and are not important sources of labile uranium. However, in the samples examined, thorite and allanite both contain uranium, some of which has been rendered potentially leachable. Thorite is partly metamict, showing typical internal fracturing due to lattice expansion, and characteristically reddened by secondary iron oxide (Plates 43 and 44). The allanite is turbid, brown and very inhomogenous (Plate 45) due to patchy metamictisation. In places this is developed to a high degree, with only rare earth carbonate remaining. Both minerals are included in primary biotite which has been altered to chlorite with the release of microcrystalline anatase, hematite (Plate 43) and possibly non-crystalline equivalents. Autoradiographic and electron microprobe study has shown that uranium has been mobilised from metamict areas and re-adsorbed locally by these amorphous or microcrystalline phases. The uraninite studied (Plate 46) also occurs in close textural association with biotite/chlorite and was found by electron microprobe analysis to contain around 10% Th. This content would be expected to reduce significantly the solubility in a low temperature weathering regime in comparison to the pitchblende from the veins.

A sample of granodiorite from near the old adit close by the Needle's Eye arch has been studied by fission track and BSEM-EDXA techniques and provides further insight in the radioactive mineral assemblage of the granodiorite margin distant from the vein mineralization. Uranium in this sample is found by fission track study to be present mainly in discrete accessory mineral grains. Highest track densities (reflecting highest relative uranium contents) are associated with subhedral crystals of thorite ($ThSiO_4$) which occur as inclusions mainly in biotite but also in plagioclase. These crystals are relatively large, up to 60μm across and typically show fractures or brecciation cracks infilled with secondary iron oxide alteration which surrounds the grains (Plate 47). Uranium is detectable by EDXA within the cores of these thorites but not in the rims and crack borders which are shown by BSEM to be less dense and contain significant phosphorus. This possibly indicates

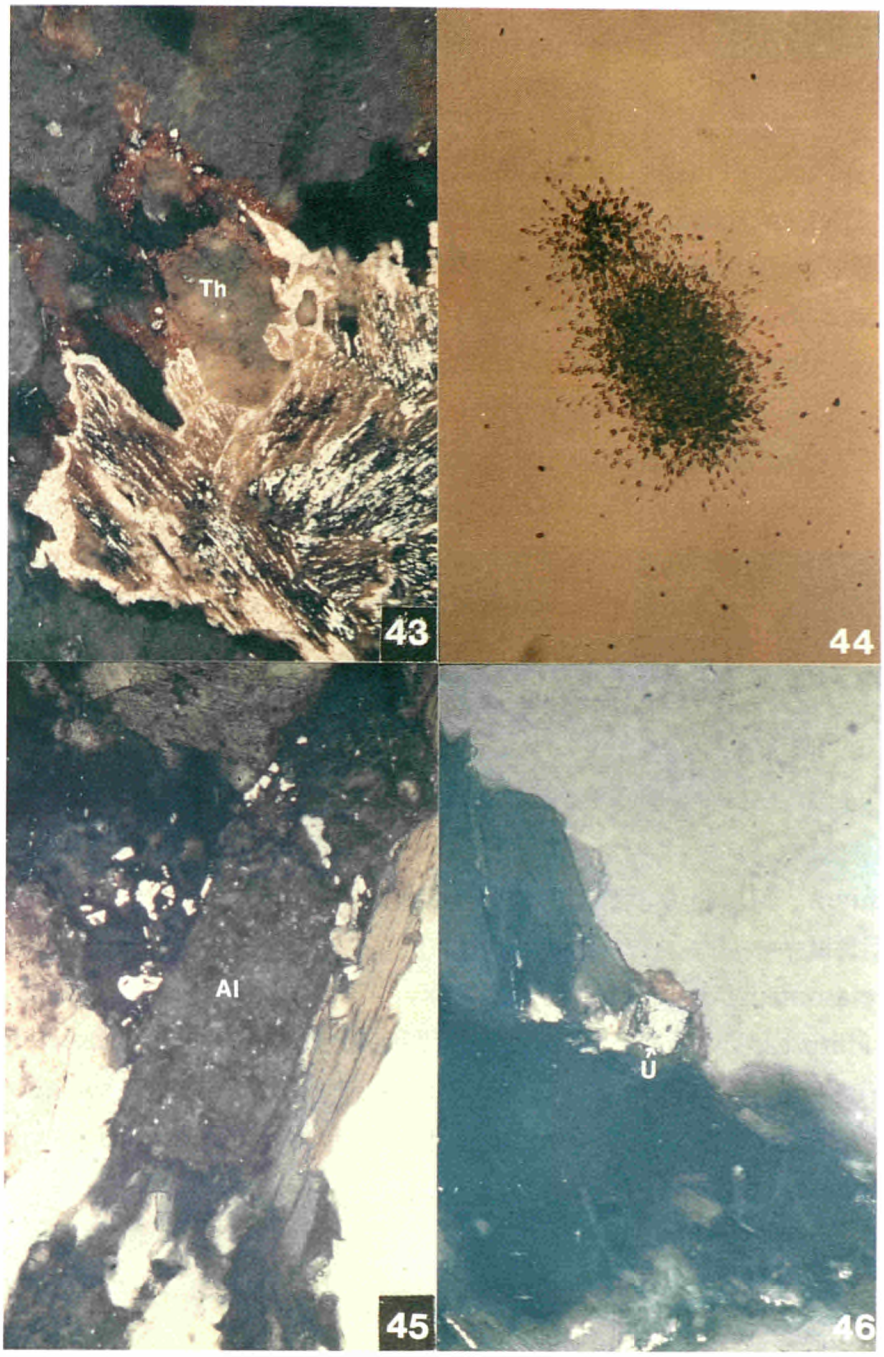

PLATE 43 Granodiorite containing partially metamict thorite (Th) with secondary iron oxide and bright reflecting hematite. Reflected light. Field width: 300μm.

PLATE 44 Autoradiograph of Plate 43 showing intense cluster of alpha tracks associated with the thorite.

PLATE 45 Granodiorite containing metamict allanite (Al). Reflected light. Field width: 300μm.

PLATE 46 Granodiorite containing uraninite (U) in association with biotite and chlorite. Reflected light. Field width: 300μm.

partial replacement by phosphate, with formation of a thorogummite-like mineral ($Th(SiO_4)_{1-x}(OH)_{4x}$).

Other relatively dense clusters of fission tracks closely relate to aggregated clusters of perfectly euhedral, tetragonal crystals of zircon and thorite (Plate 48) in a similar assemblage to that described earlier from the granodiorite wallrock (Section 4.2.1). Unlike the coarser thorite described above the thorite here does not display brecciation or appear to be either metamict or accompanied by iron oxide alteration. Neither is the zircon-thorite assemblage limited to inclusions in biotite (or less commonly, plagioclase), but instead occurs at the grain boundaries of the major minerals (in particular, quartz and K-feldspar) and appears to be a later, possibly secondary generation of mineralization. A later origin is also indicated by the occurrence of this thorite as a more phosphatic variety along immediately adjacent grain boundary cracks in quartz and feldspar and occasionally interstitially to zircons.

Less dense but discrete fission track clusters are associated with apatite inclusions and very commonly with "lozenge-shaped" pseudomorphs of anatase (Plate 49) or anatase and quartz (Plate 50) after sphene. Most pseudomorphs are associated with fine fibrous light REE phosphate (Plate 51), probably rhabdophane ($(Ce,La,Nd)PO_4nH_2O$), containing thorium and possibly uranium. Many of the quartz-anatase pseudomorphs are also associated with secondary K-feldspar, suggesting that alteration of sphene is related to the K-feldspar alteration (metasomatism) seen in the vein areas. This implies that K-feldspar alteration is probably a widespread feature in the margins of the granodiorite. The association of zircon and later thorite with K-feldspar and quartz grain boundaries and its association in the vein areas with K-feldspar of secondary origin suggests that this mineralization also is closely related to the pervasive K-metasomatism.

4.4 SILURIAN HORNFELS

The only work to date on the "background" Silurian country rocks has been confined to that described above on samples from close to the uraniferous vein mineralization. Some indication is given by study of thin sections that these rocks may contain significant levels of uranium-bearing detrital accessory minerals (Plates 39 to 42). In addition, initial field examination of the cliff section indicates that secondary dispersion of uranium on fracture surfaces or in association with oxidation products may well be widespread. More detailed evaluation is needed.

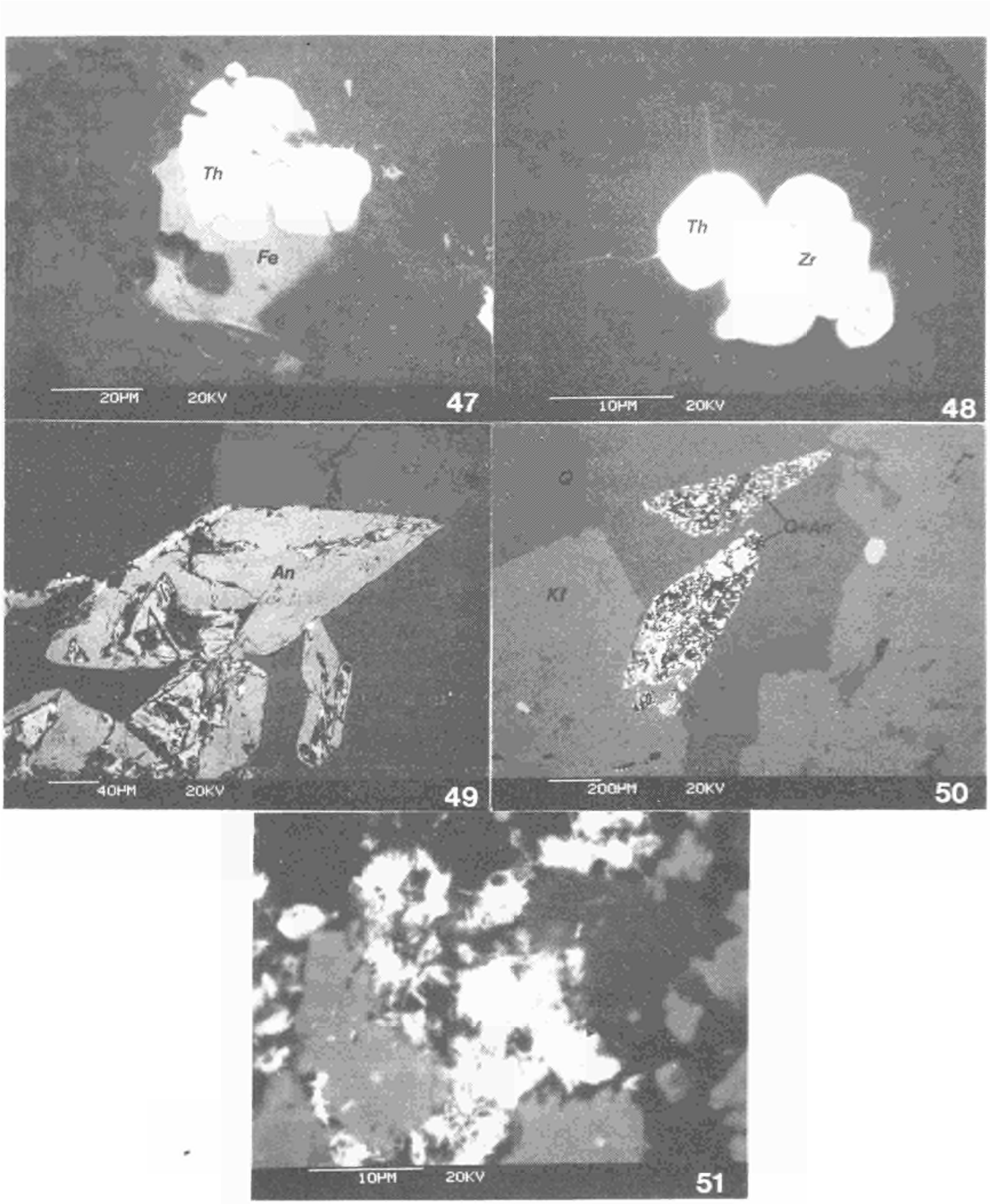

PLATE 47 BSEM photomicrograph of metamict uranian thorite (Th) associated with plagioclase in granodiorite. Note expansive cracking of thorite and secondary fine iron oxide (Fe).

PLATE 48 BSEM photomicrograph of euhedral tetragonal secondary zircons (Zr) associated with secondary low-uranium thorite (Th) at grain boundaries of K-spar in granodiorite. Note fine penetration of thorite (often slightly phosphatic) along grain boundary cracks in granodiorite indicating relatively late paragenesis.

PLATE 49 BSEM photomicrograph of anatase (An) pseudomorph after typical lozenge-shape of sphene in granodiorite. K-feldspar (Kf) and quartz (Q) also indicated.

PLATE 50 BSEM photomicrograph of complex quartz (Q) and anatase (An) pseudomorph after sphene in granodiorite.

PLATE 51 BSEM photomicrograph showing detail of quartz-anatase replaced pseudomorphs after sphene in granodiorite containing fine fibrous secondary rhabdophane or REE phosphate (RE-P).

5. QUATERNARY SEDIMENTS AND LOCATION OF URANIUM

5.1 GENERAL

Geochemical and radiometric surveys of the site have shown that significant migration of uranium from the cliff area has occurred, with secondary accumulation within the estuarine/intertidal drift sediments of the Merse. In order to study the nature of the uranium deposition and fixation within these sediments, undisturbed sediment samples were collected from two pits dug on the mudflats over the postulated position of the main uranium-bearing vein structure (Figure 2). In both cases the primary uranium structure was not encountered but significant enrichment of uranium was found in the sediments

5.2. PIT 1

5.2.1 Section

PIT 1 was dug in August 1987 in the vicinity of a high surface radiometric anomaly in the mudflat sediments adjacent to and east of the Needle's Eye arch as shown in Figure 2. The pit is also situated on the feather-edge of heaped spoil derived from an old trial adit above the site, part way up the cliff. The soil-sediment profile consists of a strongly stratified sequence of sands, gravels, silts and organic-humified materials ("peats") and is summarised in Figure 3. The drift sequence is 185 cm thick and rests directly on bedrock. However, it was not possible to sample the bedrock underlying this profile because rapid influx of groundwater below about 160cm caused the unconsolidated sand and silt to flow into the base of the pit.

At the bottom of the sediment pile about 10cm of gravel and pebbles rest on a smooth, horizontal bedrock surface. Well-rounded pebbles, up to 25cm diameter, comprise locally-derived granodiorite, hornfels and limestone with less common pebbles of vein quartz. Black and orange-ochreous staining is present on the surface of the pebbles, generally with the black stain underlying the orange skin. Similar staining is apparent within the enclosing fine to medium sand matrix, much occurring as diffuse, alternate colour bands. This pebbly layer represents a residual beach deposit and is likely to be contemporaneous with the ancient cliff line.

The pebble bed is overlain by a layer of homogenous, buff-coloured, unlaminated, fine to medium sand. This appears to be similar to the matrix of the underlying pebbly horizon but may show a fining upwards. The top (152cm depth) grades sharply into overlying grey laminated silts and fine sands. Discontinuous sub-horizontal bands and sub-spherical

patches of concentrically zoned black and orange stained sediment are present as this horizon. Locally, this staining develops as weakly-cemented concretions in the sand. Examination of these by SEM showed that the black-ochre staining and cement is due to the precipitation of fine grained, often spongey-textured, interstitial manganese-rich (black) and iron-rich (orange) oxides or hydroxides. Very localised development of pore-filling "oxide" may form a rigid cement but more commonly the oxides occur only as grain coatings. In many cases manganese coatings appear to occur close to the grain contacts and are enclosed in a film of later iron-rich "oxides", but in the pores a complex banding of iron and manganese may be present. Detrital lithic fragments of hornfels and other rock fragments may be partly replaced by these "oxides". The manganese-"oxide" precipitates contain significant EDXA-detectable iron, copper, nickel and cobalt and lesser to trace amounts of barium, zinc and arsenic. In contrast, the iron-"oxides" are enriched significantly in silicon, arsenic, calcium, copper and zinc with possible trace amounts (very close to EDXA detection limits) of thorium and REE. At this level oxidising groundwater (Eh= +235-335mV) flowed rapidly into the pit, apparently consistent with the presence of the ochreous iron-oxide staining. This sandy sediment is probably related to beach deposits representing a sandier (finer) facies of the same deposit as the pebble band.

A thick horizon of mid-grey fine sands and coarse to fine silts with darker grey clay laminae, occurs between 73-152cm and overlies the incoherent buff-coloured sands. These deposits are finely laminated and contain patches of foul-smelling (reducing) fibrous olive-grey organic matter. This material has a diffuse gradational relationship with the host sediments and appears to be largely partly-decayed plant stems and leaves (mainly grass- or reed-like) and does not appear to be associated with *in situ* root structures. It is interpreted as organic debris that drifted into the sedimentary environment during the deposition of the silts. The material was probably derived from local sources of died-back plant remains (seasonal litter) that originated on the early mudflats in much the same way that seasonal vegetation litter is developed on the present day mudflats, being then removed and redeposited with tidal inundations. The grassy or reed-like nature of this material is similar in character to the vegetation seen on the modern mudflats. Abundant fine, partly-decayed, subvertical rootlets are abundant in the silts, particularly towards the top of the unit, the upper 10-15cm being transitional into the overlying peaty horizon. These rootlets are i*n situ* and the enclosing root channels are surrounded by diffuse black haloes. These laminated silts are interpreted as having been deposited under conditions similar to the present day intertidal estuarine mudflats.

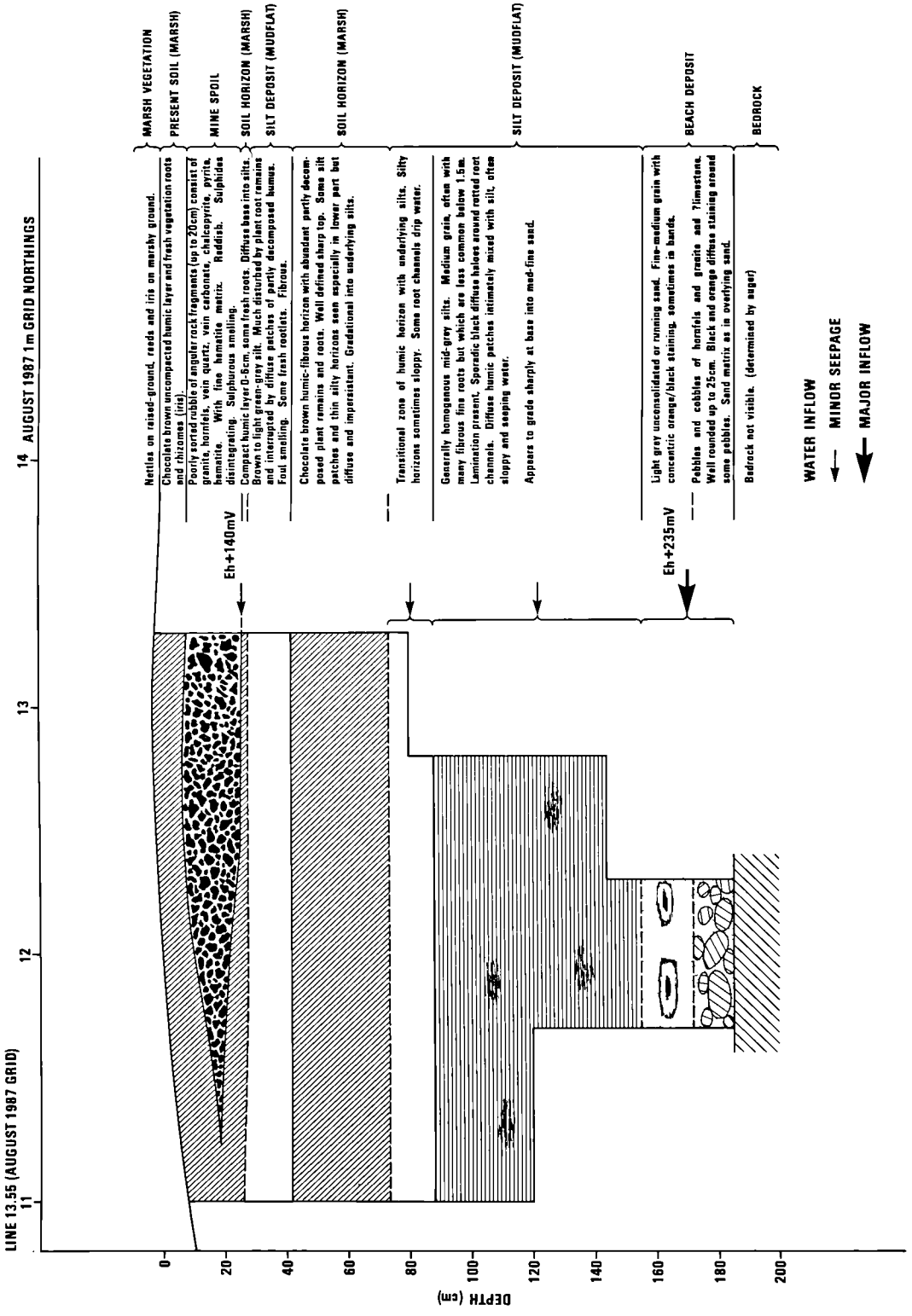

Figure 3: Schematic sediment-soil profile of PIT 1, showing depth and Eh of prominent water inflows.

Between 42-73cm depth a well-humified chocolate-brown organic or peaty horizon is developed. The top 10-15cm of the underlying silts are gradational into the "peat" and appear to have been reworked by the process of peat formation, leaving residual traces of laminated grey silt within the organic horizon. This layer is interpreted as an ancient soil horizon, probably developed in a similar manner to the modern boggy soils at the present location. Within the peat, partly decomposed plant remains are abundant and the horizon is foul-smelling, indicating reducing conditions. The transitional zone between the peat and underlying silts is very incoherent and in places in a near-fluidised state.

A thin horizon of laminated brown-grey silt between 28-42cm depth overlies the peat horizon. The junction with the underlying peat is very sharp but the silt horizon itself is gradational upwards into the overlying modern soil. Modern (living) roots and partly humified root remains are abundant and have significantly disturbed much of the lamination in the sediments. As in the lower silt unit, diffuse patches of rafted organic matter are common. This silt horizon is interpreted as having been deposited after a slight rise in the sea level inundated the early peat bog and led to a brief period when the area of active mudflat sedimentation extended to the base of the cliffs.

The bulk mineralogy of the silts has been described previously from both the peat bog area and further out in the mudflat deposits (Hooker *et al*, 1986). The silty sediments are composed dominantly of detrital quartz (c.50%) with major detrital plagioclase, K-feldspar, mica (including illite clay minerals), and chlorite. Organic carbon contents vary considerably (c. 5-80%) as might be expected, depending on the lithology (i.e. peat or silts). In addition to the manganese/iron concretions discussed above, diagenetic effects recorded in the sediments are the precipitation of framboidal pyrite in association with decaying organic remains in the silt and the older peat horizon, minor dissolution of K-feldspar and plagioclase in the basal sands and silts, and the corrosion of detrital ilmenite accompanied by its replacement by iron-oxides.

A thin organic-rich peaty soil overlies the silt and has been buried and compacted beneath heaped-up hematitic mine spoil, a thin wedge of which was penetrated by PIT 1. Loosely compacted, waterlogged, fibrous modern organic soil overlies the mine spoil for 10cm. A slow but steady seepage of water was noted at the base of the spoil which was found to consist of a rubble of granite, hornfels, vein quartz, vein carbonate, chalcopyrite, pyrite and hematite fragments in a fine hematitic matrix. The sulphide fragments are actively disintegrating and the freshly disturbed spoil has a sulphurous smell. This soil horizon developed after the sea level fell to its present position and conditions once more favoured the formation of a peat-bog at the base of the cliffs.

The evidence described above from PIT 1 indicates that fluctuations in sea-level have occurred at the Needle's Eye site with the result that the environment near the cliff has changed from beach to mudflat/estuarine to peat-bog, with a brief return to mudflat conditions before the resumption of the present-day peat bog environment. This change in environment will have had a significant effect on the geochemistry of the site and the groundwater conditions in the past. It may be possible to correlate these changes in sea level and the associated older peat horizon with similar horizons developed at Kirkcudbright Bay and New Abbey when the sea-level was at a lower level than present (Goodlet, 1970).

5.2.2 Location of Uranium

5.2.2.1 *Primary Locations*

Uranium bearing detrital minerals occur fairly uniformly throughout the sediment profile, and the variety of fission track densities suggests that several mineral species are present, too small to be specifically identified optically. Preliminary BSEM observation indicates that these minerals include zircon, apatite and anatase associated with amorphous secondary light REE phosphate (? rhabdophane). Although no uranium could be detected by EDXA, these minerals are likely to contain a considerable range of uranium contents from a few tens to several thousands ppm (Basham *et al*, 1982). It is most probable that the detritals have been derived from local country rocks and correspond with "primary" site minerals mentioned earlier, although the regional pattern of sediment transport into the Solway Firth from the Irish Sea (Cronan, 1969) may complicate the assemblage. The process of erosion and deposition may well have rendered them more susceptible to leaching than their equivalents contained in the host lithologies.

5.2.2.2 *Secondary Enrichment*

Examination of fission track prints indicates that most of the uranium in the sediments is located within organic material. Concentrations occur at two distinct levels within the profile - between 30 and 60cm depth and below about 100cm - corresponding to the two peaks for uranium in the geochemical profile obtained by XRF analysis reported by Roberts *et al*, (1988, Figure 5) and further illustrated in Figure 4.

In the uppermost horizon fission tracks are concentrated within fine grained organic matter in the sediment matrix and are strongly enhanced around root channels (Plates 52 and 53) and in sub-horizontal bands (Plate 54 and 55). Estimation of uranium concentrations from track counting in comparison with uranium glass standards shows that concentrations in fine

organic peat matter around root channels are frequently in the order of several hundred ppm uranium, whilst the "background" peat generally has levels of less than 5ppm uranium.

Uranium is not present in sufficient quantities to be detectable by BSEM-EDXA but SEM study of root surfaces and associated soil particles from one of the most prominent plants growing in the area, Yellow Flag Iris (Iris pseudacorus), revealed the presence of uraniferous minerals. These include prismatic, platy or fibrous phases containing uranium-arsenic (possibly troegite) and uranium-arsenic-copper (?zeunerite, $Cu(UO_2)_2(AsO_4)_2.10\text{-}16H_2O$) (Plate 56) and rarer, fine structureless (c. 0.2-1μm) subspherical uranium-bearing particles (possibly an oxide eg uraninite or hydrous phase) which coat the root surface. A less common uranium-bismuth-copper-arsenic (±Si-Al-Ca-Ti-Mn-Fe-Ni) phase is also present. Many of these phases appear to nucleate on and within the root surface organic membranes (Plate 57). Root surfaces of the Great Wood-rush (Luzula sylvatica) growing in soils directly over the mineralization in the cliff were also examined and found to contain similar uranium-arsenic minerals. In both cases associated spongy or fine grained iron and manganese oxides may also be present and may contain significant contents of other metals including lead, zinc, copper, arsenic and cobalt.

Observation of the soil sections indicates that fine grained framboidal pyrite, common throughout the peat, is less common in areas of uranium accumulation suggesting that oxidation has occurred. The presence of orange iron oxidation haloes around many root channels also suggests that uranium may have been transported in solution through open root channels (mainly vertical) before being complexed onto surrounding organic material in the peat. The nature of this complexing has not yet been characterised. It may simply be an association with amorphous iron oxides, but a possible relationship with metal-fixing mycorrhizal fungi (i.e. fungi living in symbiotic association with plant roots) around the roots cannot be ruled out since fungi are known to significantly and selectively concentrate uranium (Nakajima and Sakaguchi, 1986). In the sections, individual root channels frequently extend >5cm and appear to be interconnected. The absence of uranium from some (identical) roots suggests that either only some were active at a particular period of uranium mobility, or that only specific root systems were tapping the uranium "source". Textural reorientation of the peat matrix by root activity significantly enhances the permeability around the root stem.

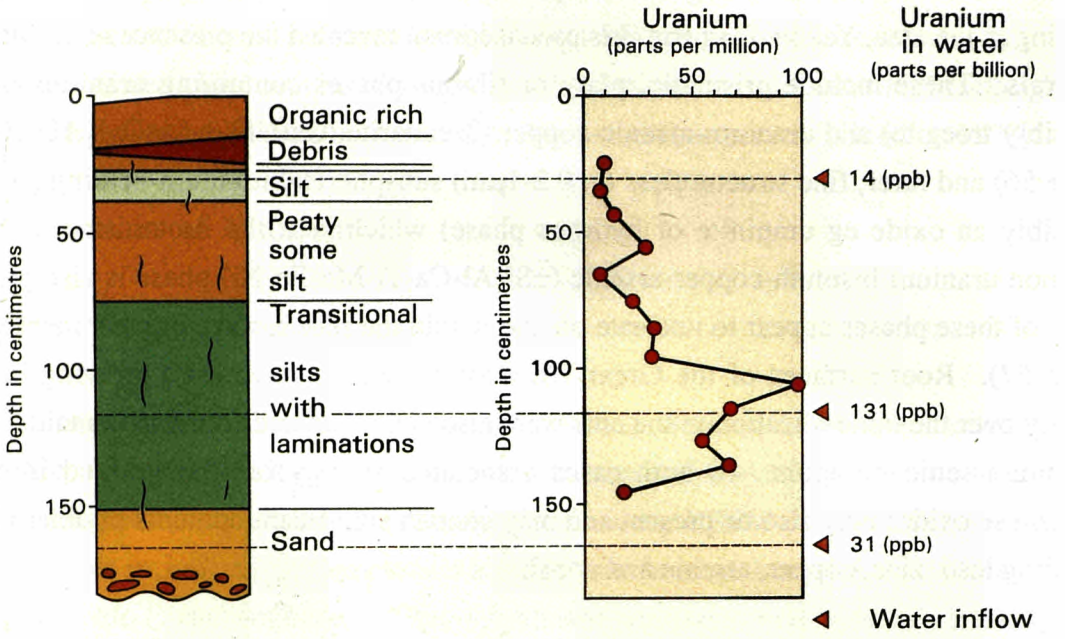

Figure 4: Distribution of uranium in sediment and groundwaters from PIT 1 (from Roberts *et al*, 1988).

In the deeper location of uranium enrichment fission tracks are almost exclusively contained within organic plant debris in the silts, in particular large plant roots (Plates 61 and 62). Track density is often higher in specific parts of the root, notably the vascular bundle in the centre and the darker wall material or exodermis (Plates 63 and 64). Close examination of the root structures identifies most as a monocotyledon identical to that of Iris (Shaw *et al*, 1965). BSEM-EDXA indicates that the cell walls of certain structures in the vascular bundle are enriched in various elements (Plate 58). In particular the walls of pith cells are enriched in aluminium, sulphur, calcium and iron with minor concentrations of silicon (Plate 59). The walls of endodermis cells, comprising the endodermic ring around the perimeter of the vascular bundle, are likewise enriched but also contain significant concentrations of cobalt, copper, and possibly zinc and nickel (Plate 60). A similar association is seen in the cell walls of the exodermis (the layer beneath the epidermis). Uranium is just detectable by EDXA in the pith and endodermis cell walls indicating that levels of enrichment must be of the order of 1000-5000ppm, which is consistent with estimates from fission track density. Tiny needle-like mineral precipitates (silica, alumina, aluminium-silicate) commonly occur at cell junctions in the cortex region, perhaps representing ergastic substances (e.g. Esau, 1960), but do not appear to relate to the uranium distribution. Within a plant structure, uranium abundance is highly variable from less than 5ppm to several hundred ppm commonly, and often to over 500ppm in the central columns. Uranium accumulation again appears to be controlled by water flow through root material which, even when dead or detrital, may still provide permeable pathways. The ability of organic matter to fix mobile uranium is also a significant factor.

At both horizons of uranium enrichment, uranium has a particular affinity for darker coloured plant debris, black carbonised fragments (Plates 54 and 55) and porous spore material. Estimates of uranium contents by track counting based on comparison with calibrated standards gives values of 30-80ppm for sediments in the upper level and approximately 100ppm for the deeper concentration. These figures correspond well with the values given by Roberts *et al*, (1988) and indicate that most of the uranium budget in the sediments can be accounted for by this organic association.

Fission track prints show that small concentrations of uranium are associated with the fine iron-manganese-oxide staining and concretions in the sandy base of the profile. In mass balance terms, this oxide-fixed uranium is probably of minor significance but nevertheless the association may indicate the potential of the iron-manganese oxide precipitates around some root channels as sites of secondary uranium deposition.

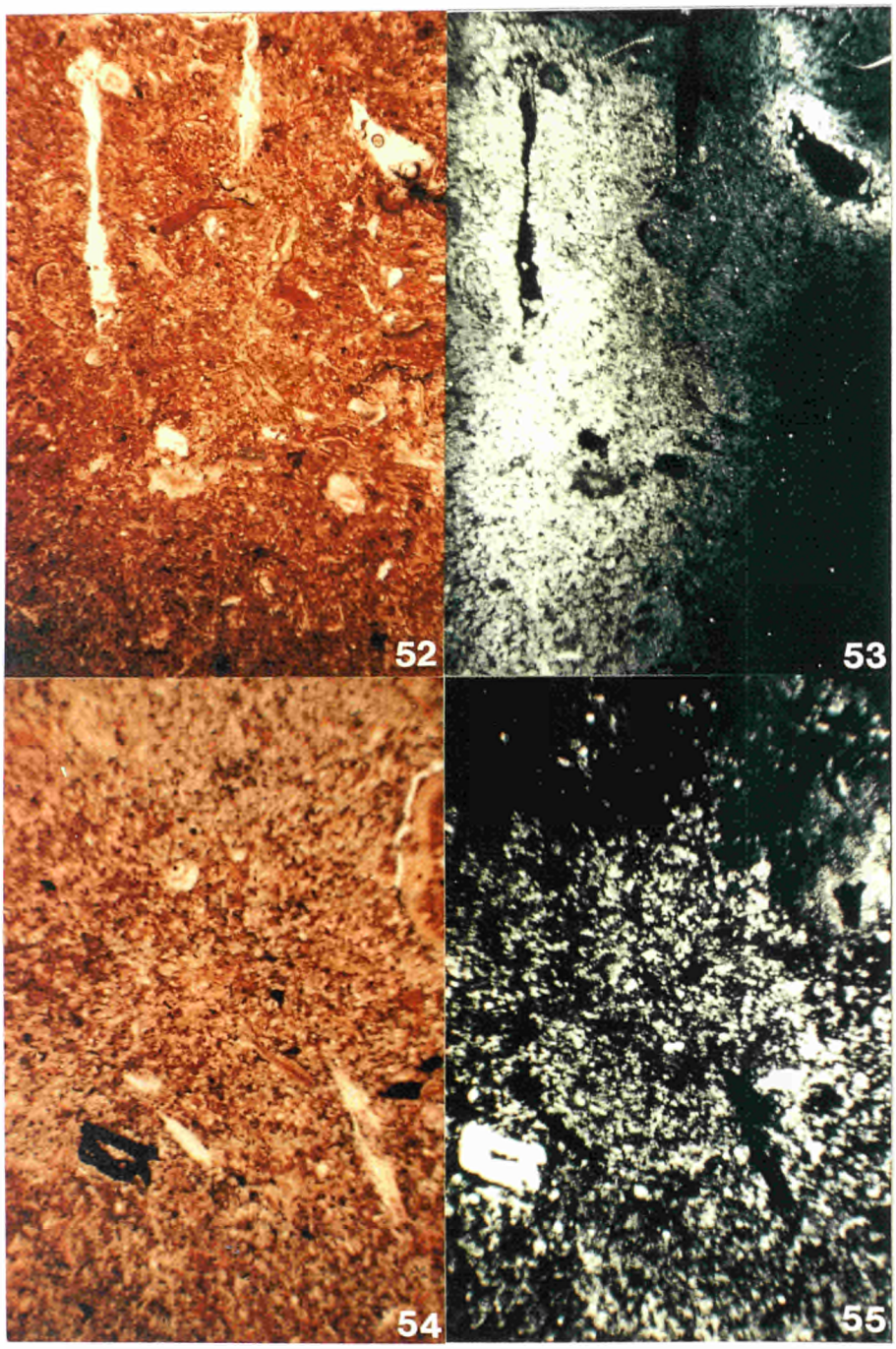

PLATE 52 Organic-rich sediment from PIT 1 at 40cm depth. Plain transmitted light. Field width: 7mm.
PLATE 53 Fission track print of Plate 52 showing uranium dispersed around root channels, contained within fine organic matrix material.
PLATE 54 Organic-rich sediment from PIT 1 at 42cm depth. Plain transmitted light. Field width: 7mm.
PLATE 55 Fission track print of Plate 54 showing uranium dispersed in a sub-horizontal band, located within fine organic matrix material. Note intense concentration in black carbonised debris.

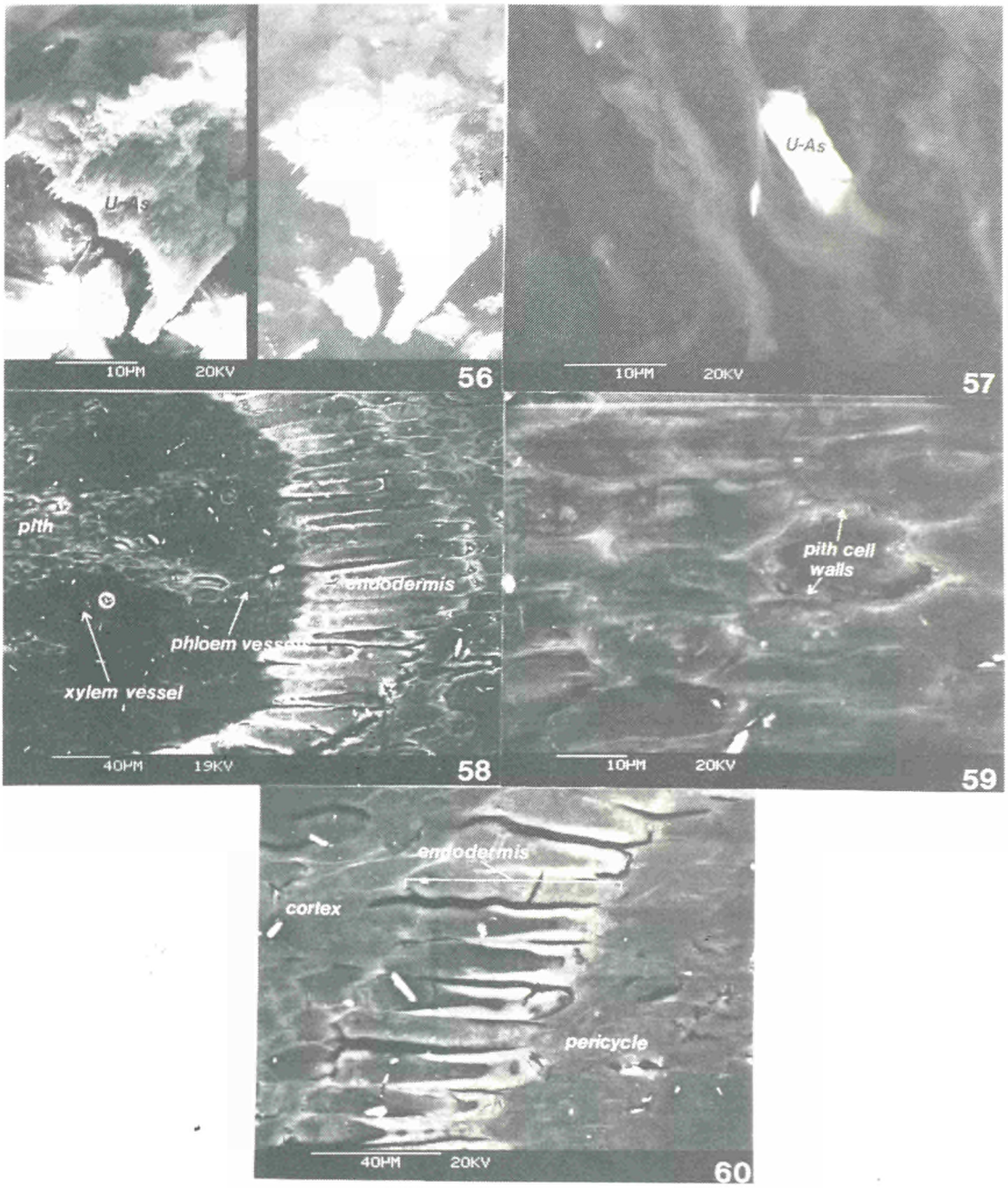

PLATE 56 BSEM photomicrograph of fibrous uranium-arsenic mineral, possibly troegerite (U-As), growing on the surface of a living iris rootlet from surface soil in peat bog.

PLATE 57 BSEM photomicrograph of platey uranium arsenic mineral, possibly troegerite (U-As), precipitated within and replacing cell walls at the surface of a living iris rootlet from surface soil in peat bog.

PLATE 58 BSEM photomicrograph of section through vascular bundle of iris root from deeper peat horizon in PIT 1 at 102cm depth showing metal enrichment of cell walls of pith cells and unicellular endodermic ring resulting in brighter image (cf same feature in Plate 63).

PLATE 59 BSEM photomicrograph of pith cells in Plate 58 showing brighter (metal enriched) cell walls.

PLATE 60 BSEM photomicrograph of endodermis of iris root in Plate 58 showing thickening (lignified) of endodermic cells on inner side of endodermic ring. This thickened region is enriched in metals and consequently shows bright on BSEM images.

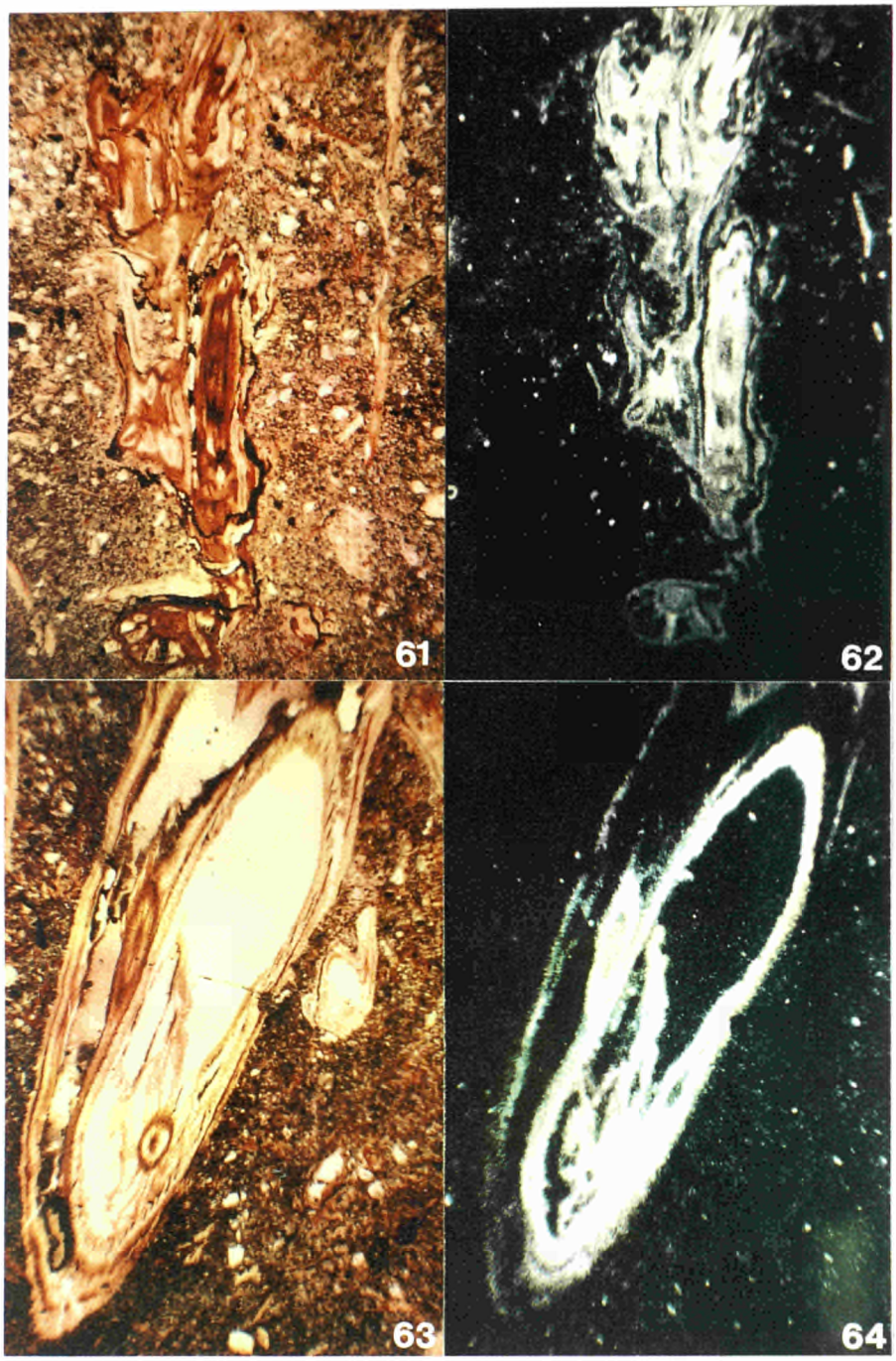

PLATE 61 Large vertical root stem in silty sediment from PIT 1 at 143cm depth. Plain transmitted light. Field width: 7mm.

PLATE 62 Fission track print of Plate 61 showing concentration of uranium within plant root and other large organic fragments.

PLATE 63 Cross-section of a root stem from PIT 1 at 102cm depth. Plain transmitted light. Field width: 10mm.

PLATE 64 Fission track print of Plate 63 showing strong concentration of uranium within specific parts of the plant structure.

5.3 PIT 3

5.3.1 Section

PIT 3 was dug in November 1987 in a further attempt to locate the "source" mineralization beneath the mudflat sediments. This pit was also located near to the Needle's Eye arch but approximately 10m further seawards from PIT 1 (Figure 2). Primary mineralization was not encountered and the sediments lie directly on unmineralized Carboniferous Limestone Series bedrock, samples of which were collected for characterisation during the next phase of the study. Similarly to PIT 1, PIT 3 is also situated on the feather-edge (seaward side) of the heaped spoil derived from the old trial adit in the nearby cliffs. The drift sequence encountered was 165 cm thick and beneath a thin layer of spoil debris the soil profile consists largely of fine grained laminated grey silts with interbanded thin brown organic-rich bands, generally less than 1cm thick. The profile examined is summarised below:

The base of the sediment profile (165cm depth) rests on smooth bedrock comprising an inclined bedding plane of hard, black, dense recrystallised silty limestone or calcareous siltstone. The limestone/siltstone carries occasional irregular fine veinlets of white calcite typically of the order of 1mm wide but no obvious major mineralization could be discerned nor was the bedrock noticeably radioactive. The bedrock gave a strong sulphurous smell when freshly struck. A slow water seepage was observed at the interface between the bedrock and the overlying drift sediments.

The sediments overlying the bedrock between 116-165cm depth comprise a generally homogenous sequence of grey clay-rich fine silts with coarse laminations. Scattered horizontally orientated patches of foul-smelling (reducing) fibrous olive-brown organic matter (matted and decayed reed or grass-like plant stems and leaves) are present and are interpreted as drifted organic detritus deposited with the estuarine mudflat silts (cf. PIT 1; section 5.2.1). Black, carbonised plant remains penetrating through the laminated sediments were also identified and represent *in situ* root remains.

Between 71-116cm depth the silts appear to pass gradationally into more finely laminated material and upwards gradually display orange or ochreous mottling. This mottling appears to be developed around former root channels and was particularly evident in a zone between 85-100cm depth. Diffuse black-stained patches of silt were observed. Soft black carbonaceous material occurs as dispersed flecs and as material infilling former root channels were identified. Many of the old root channels slowly seeped water in the exposed soil pit walls.

Above about 71cm depth the grey silts pass up into homogenised brown-grey fine silts. The silts display well-developed ochreous mottling and also less abundantly developed diffuse patchy black staining. Root channels are common and both living and decomposed roots are present at this depth. Many of the fine root channels occupied by soft black decomposed plant remains are surrounded by a haloe of ochreous staining. The silts display no obvious lamination at this depth, the lamination possibly having been lost as a result of more extensive disturbance by plant roots.

At about 36cm depth the grey-brown silts are overlain by a thin hematitic rubble of mine spoil containing a similar assemblage of materials to that described from PIT 1 (section 5.2.1) and includes rotted sulphide ores, granodiorite and hornfels fragments. A thin modern red-brown organic soil has developed over the mine spoil (0-21cm depth).

Even though the two pits are only 10m apart the soil profile encountered in PIT 3 is significantly different to that described from PIT 1; the prominent organic-rich peat horizon seen in PIT 1 is absent in PIT 3. In this respect the difference between the two pits mirrors the present day soil-type distributions at the two sites. The area around PIT 1 comprises a peat bog developed in an area of upwelling groundwater associated with springs at the base of the cliffline. Beyond about 20-25m from the cliffline the groundwater is no longer upwelling and the terrain is better drained and the peat-bog conditions disappear. Consequently, PIT 3 is beyond the range of the present day peat bog conditions and it would appear from a comparison of the two profiles that this has also been the situation in the past. A further difference between the two pits is the lack of a permeable pebbly-sandy horizon at the base of the section in PIT 3 which may be the result of the site being further from the cliffs (beach line). This results in significantly less groundwater influx compared to PIT 1.

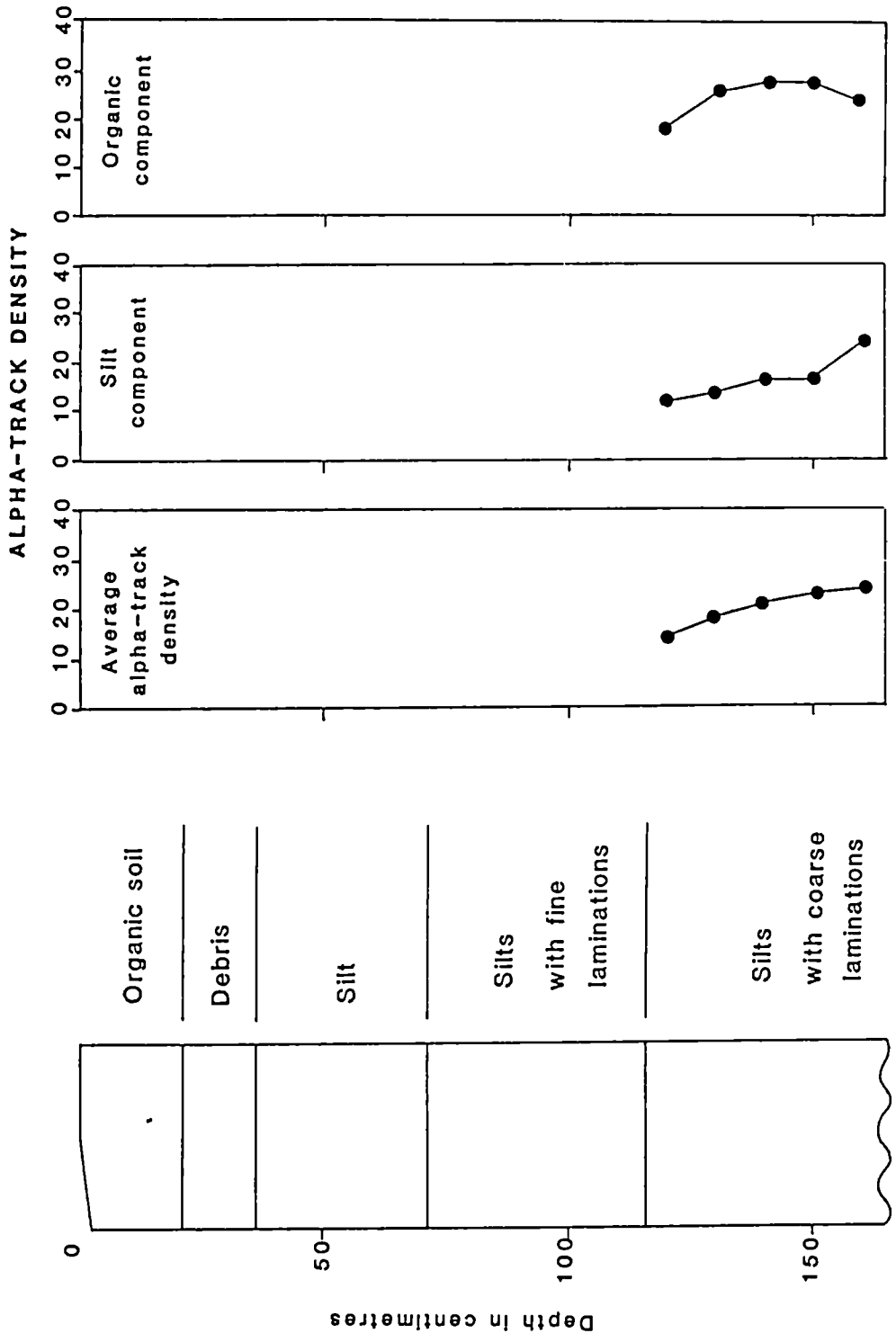

Figure 5. Schematic sediment-soil profile of PIT 3, showing radioelement distribution estimated from autoradiography.

5.3.2 Location of Uranium

Autoradiograph alpha-track registration for samples in the lower half of the pit indicates a progressive increase in alpha particle activity towards the base of the sediment profile (Figure 5). Within each sample most of the tracks are located within the organic bands and seem to be concentrated within the fine matrix organic matter in the sediments in a similar way to the upper parts of PIT 1. Thus, again, the distribution of radioelements is strongly linked to organic matter in the sediments. No SEM analyses have been performed on samples from this pit.

Overall track density is generally less than half that of PIT 1, indicating that uranium is considerably less abundant. This suggests that the uranium transported in solution from the source area is efficiently retarded by the organic matter fringing the cliff base, and relatively little is transported further seawards. The increase of activity at the base of the pit may indicate input of radioelements from groundwater influx along the sediment-bedrock interface. As noted earlier, this flow is considerably less than in PIT 1 which may explain the lower concentrations of radioelements.

6. DISCUSSION

6.1 GENERAL

Selection of the Needle's Eye site for study in the natural analogue programme was made on the basis of the work of Miller and Taylor (1966), which demonstrated the presence of a highly leachable source of uranium in the pitchblende mineralization in the cliffs and radiometric evidence of dispersion into the silty sediments of the mudflats. The samples examined in this study were collected specifically to confirm this earlier work and to examine in more detail mineralogical features of release, transport and redeposition mechanisms.

6.2 SOURCES OF URANIUM

Uraninite has been confirmed as the main host for uranium in the veins by virtue of its frequency of occurrence and high uranium content. It is present as the low temperature, botryoidal variety pitchblende and, in keeping with this style of occurrence, is characteristically low in (or devoid of) thorium and readily affected by weathering (Frondel, 1958). The dominance of carbonates as the gangue in the veins indicates that uranium will be readily transported from source as the uranyl carbonate complex. The polymetallic character

of the associated mineralization is reflected in a variety of sulphides, arsenides etc. which are likewise relatively unstable in the supergene environment, becoming oxidised and giving rise to a large number of complex secondary minerals. The ability of hexavalent uranium to combine with a wide range of cations and anionic complexes (eg phosphate, arsenate, vanadate, silicate hydrate) results in redeposition of uranium as secondary minerals in close proximity to source. The composition of these minerals may vary within a short distance, reflecting local availability of formative elements. Often two or more minerals occur together in close textural association. This study has recognised several such secondary uranium minerals within the veins themselves and in fractures in the adjacent wallrocks. Although boltwoodite (hydrous potassium uranium silicate), zeunerite (hydrous copper uranium arsenate) and uranophane (hydrous calcium uranium silicate) are the products of *in situ* alteration of pitchblende recorded by Miller and Taylor (1966), a number of additional minerals have been recognised in this investigation. Within the vein, simple uranium silicate(s) (coffinite or soddyite) occur in close association with surfaces or oxidation products of the sulphides, mainly chalcopyrite, and similar phases are found to a minor degree associated with cracks in hydrocarbon globules. Textural relationships indicate that it is possible that these minerals could have formed as part of the "primary" mineral paragenesis.

Further support for this is given by the occurrence of aggregates of well-formed platy crystals of a uranium-arsenic mineral (possibly troegerite) enclosed in quartz-feldspar veinlets in the hornfels siltstone wallrock. Development of "secondary" minerals in these locations could relate to the pervasive wallrock alteration which is seen in the enclosing siltstones and granodiorite. In the case of the latter, early quartz-adularia alteration at the vein margin appears to have affected primary uranium-thorium-REE-bearing accessory minerals including thorite and monazite. Secondary development of xenotime, zircon, thorite-uranothorite and ?rhabdophane reflects either redistribution from the primary phases or introduction of contributing elements in early (higher temperature) mineralizing fluids. On a more regional scale, the granodiorite shows similar evidence of early potassic alteration associated with reprecipitation of thorium silicate (thorite), the secondary form of the latter being distinguished from the primary accessory form by its finer grain size, absence of metamictisation and close textural association with secondary zircon. The limited work done so far on the "background" granodiorite therefore demonstrates the presence of uranium-thorium-REE accessory minerals, some of which appear to have been mobilised and redistributed locally by hydrothermal (metasomatic) processes which may relate to the widespread vein mineralizing episodes. Further evidence from fission track analysis shows that uranium has been redistributed into sites of alteration of other minerals, for example anatase pseudomorphs after sphene and hematitic alteration of biotite and chlorite. These fine

grained and poorly crystalline or amorphous hosts may be considered as susceptible to further remobilisation under contemporary supergene leaching conditions. Therefore, in assessing the input of analogue elements into the waters draining the cliff from the vein mineralization, the potential of the host rocks as contributors to the "background" hydrogeochemistry should also be considered. Indeed, it may be that the granodiorite could provide a useful "source term" for modelling thorium series and rare earth analogue elements at the site.

Considering the recent to present-day weathering regime, ample evidence exists of the leaching of uranium and redistribution into secondary solid-phase sites within the cliff rocks. Despite the suggestion made above that some of the so-called "secondary" uranium minerals may have formed at an earlier stage related to the ore mineral paragenesis, most of the secondary minerals which coat fracture surfaces in the vein and wallrocks up to some distance from the vein are recent. They are frequently associated with the products of supergene alteration of the sulphides, particularly the abundant copper secondaries, and include calcium-arsenic, magnesium-arsenic and silicate uranium minerals. In addition, uranium is commonly adsorbed to relatively high levels by iron oxide weathering products of the sulphides. The latter mode of occurrence seems particularly prevalent within the hornfelsed siltstones, related to the common fine sulphide veinlets present in the pervasive fracture networks.

6.3 HYDROCARBON

Previous workers have proposed the hydrocarbon in the veins as an important host of uranium (Miller and Taylor, 1966; Parnell, 1988; Eakin, 1989). In contrast, this study has shown that insignificant levels are contained intrinsically within the hydrocarbon phase itself although trapped grains of discrete uraninite, reported in other studies, are not excluded. However, it is to be noted that chemical dissolution studies indicate that the hydrocarbon has low solubility in the present supergene environment and it is therefore unlikely that any contained inclusions of uraninite would be easily dispersed by groundwater reaction.

Of much greater interest to the present considerations of uranium mobility and fixation is the evidence found of biological alteration and uranium mineralization of hydrocarbon when exposed to weathering and soil-forming processes. Well-preserved structures observed by SEM on exposed surfaces and open fractures are indicative of microbial activity. Weathered uranium ores from the Westphalian of the Vosges have previously been reported to contain bitumens carrying viable cocci- and bacillus-type bacteria with uranium contents in excess of 10% dry weight (Capus and Munier, 1978). Accounts of naturally uraniferous bacteria are

rare, however, microbial influences are often considered to be important in the formation of hydrocarbon-related uranium deposits (eg Landais, 1989) and secondary supergene uranium mobilisation and redistribution (eg Magne *et al*, 1974) where microbial biodegradation of organo-uranium complexes may promote neoformation of uranium deposits.

In the case of the Needle's Eye bitumens, the appearance of the structures resembles fungal filaments but many of the features more closely resemble the actinomycetes (J. West, pers.comm.), a group of bacteria which develop filamentous structures with fruiting (sporing) bodies. Varieties of these are abundant in soils, are known to mineralise hydrocarbons and have a highly selective affinity for uranium (Nakajima and Sakaguchi, 1986). Different element associations have been noted in different sites in the organisms present here, including uranium, selenium, bismuth and other elements known to be present in minerals in the veins. Uranium itself is largely associated with the cell walls. The uptake of uranium and other heavy metals by bacteria has been described from natural systems (Degens and Venugopalan, 1982) and experimental studies (Beverage *et al*, 1983) and specific concentration in the cell walls is considered to be due to the unique presence of specially developed surface active structures and functional groups (Francis and Beveridge, 1985). Preliminary culturing from hydrocarbon fragments on media suitable to encourage growth of actinomycetes has produced filamentous organisms of similar appearance (but without obvious fruiting bodies) suggesting that the bacteria in the hydrocarbon fractures are viable. The presence of these, and the evidence of their strong ability to absorb and concentrate heavy metals from the active groundwaters draining the mineralization, may give clues to more widespread associations and processes in the secondary environment at the site.

6.4 SECONDARY SITES OF URANIUM CONCENTRATION

Study of radioelement distributions in undisturbed samples from soil and sediment profiles in the Merse silts by the sensitive techniques of autoradiography and fission track registration has shown that uranium is strongly associated with organic matter. Close correlation was found between the highest concentrations indicated by these techniques and those determined by chemical analysis of bulk samples. The two "highs" thus indicated in PIT 1 also correspond fairly well with horizons of high lateral water flow as determined by hydrological measurements at the site.

In the upper, well-humified "peaty" part of the profile in PIT 1, sub-horizontal organic-rich bands are fairly uniformly enriched in dispersed uranium. Open root channels show haloes of enrichment to one or two orders of magnitude over the 5ppm level measured in the general

matrix. This enhancement in uranium content appears to relate to the local oxidation of iron (present in the matrix as pyrite), and transport of uranium into the sediment in oxygenating groundwater is therefore indicated, with fixation by amorphous iron. However, the role of biological activity has not been fully established in this context and metal-fixing mycorrhizal fungi may be present around the roots. Study of living root surfaces by SEM has revealed the presence of a number of very fine, uranium-bearing mineral precipitates including phases containing in addition arsenic, copper-arsenic and bismuth-copper-arsenic. Iron and manganese are also commonly associated, along with a number of the other metallic elements characteristic of the vein mineralization.

Uranium also occurs in an adsorbed form associated with iron or manganese concretions or weathering skins on clastic fragments within the soils. The levels of uranium in these sites are low compared with those attained in fragments of carbonised organic debris which occur throughout, and are not considered to be important sites of accumulation in quantitative terms.

Deeper in the profile examined in PIT 1, uranium is contained mainly within plant roots, in particular those of Iris which is a common plant growing at the site at present. Fission track registration has shown that uranium is concentrated in certain parts of the plant structure and SEM examination has shown these to be mainly the areas with specially thickened cell walls associated with control of water movement within the plant. Pith cells in close proximity to the vascular bundle also show concentration. The association of uranium with structural members of the water control system suggests that uptake of uranium occurred in the living plant. In this respect the observations resemble those of Apps *et al,* (1988), who when studying living grasses (also monocotyledons) growing on uraniferous mine spoil, found similar and startling concentrations of uranium in a sheath zone around the vascular cambium of roots. Although it is known that certain parts of plants (eg leaves, roots) can concentrate uranium, detailed understanding of sites and fixation processes is lacking. In the example here, if uptake and concentration has taken place in the living plant, the occurrences in this lower horizon are "fossil" features, as the rooting system of Iris is shallow and the preserved structures at this level are buried remains. An alternative explanation, but perhaps less credible, is that absorption by more humified parts of the plant material has occurred. In this case uptake could be an active feature of the present-day hydrogeochemistry.

Comparison of relative radioelement concentrations and distributions indicates that at least a 50% reduction has occurred between PITS 1 and 3. This suggests that the organic matter fringing the cliff base has formed an effective retardant to uranium being transported seawards in groundwater. Although most of this is probably fixed in organic complexes, an

indeterminate amount has been deposited as extremely fine, complex inorganic phases similar in composition to secondary uranium minerals (mainly, or at least including, arsenates).

Very fine-grained uranium-bearing detrital minerals are present throughout the silts but are not thought at this stage to represent a significant proportion of the total uranium content.

7. CONCLUSIONS

As a result of detailed mineralogical study of samples of vein material, granodiorite and siltstone wallrocks from cliff exposures and undisturbed material collected from two pits dug in the estuarine/intertidal sediments of the Merse, the following conclusions can be drawn regarding the "source-term" and "sink-term" at the Needle"s Eye natural analogue site:-

1. The most important source of readily mobilised uranium in the cliff section is the uraninite (variety pitchblende) in the polymetallic-carbonate breccia veins. Evidence of the effects of contemporary weathering is seen in the presence of abundant secondary minerals, mainly arsenates and silicate-hydrates, and in the absorption of uranium from groundwater by ferruginous weathering products of sulphides in the veins and iron-rich silicates in host-rocks. Together with similar "secondary" minerals considered to have formed as part of the vein mineralization, these uranyl phases present a minor, but widespread ancillary source of uranium.

2. Vein hydrocarbon, cited by previous workers as uraniferous does not, in itself, contain labile uranium and, as it is considered to be relatively stable in the present supergene environment, is unlikely to release significant uranium from any discrete included uraninite.

3. Wall-rock alteration and pervasive fine mineral veining has affected both granodiorite and hornfelsed siltstone host rocks. One effect has been to create a primary dispersion halo of metal enrichment around the main "source-term" vein from which uranium might be mobilised to a lesser degree. A second effect, associated with pervasive potassic alteration and feldspar development, has been the alteration, remobilisation and redeposition of a number of primary accessory minerals in the granodiorite as finer-grained uranium-thorium-REE silicates and phosphates. Together with metamictised primary thorium and REE minerals, these present possible "source-terms" for modelling mobilisation and transport of the thorium-series and rare earth analogue elements and are worthy of further study in this respect. Limited preliminary analysis of granodiorite some distance from the Needle's Eye vein indicates that these features may be present on a more regional basis. In any case,

modelling of the transport of uranium series elements in the cliff waters should not exclude the possibility of input from the cliff rocks, additional to that from the vein pitchblende.

4. In the secondary environment at the site, evidence has been found of the effectiveness of micro-organisms associated with exposed fracture surfaces on hydrocarbon in concentrating uranium and other metallic elements mobilised in groundwaters from the mineral veins. These features indicate the mineralizing potential of bacteria and other microorganisms in the soil regime at this site and suggest that further investigation of the extent of such retarding mechanisms is warranted.

5. Uranium being carried seawards by groundwaters from the cliff area has been shown to be effectively retarded by organic matter in the silts and peaty soils on the Merse. Fission track techniques have demonstrated convincingly the strong correlation of uranium with both semi-amorphous, humified (peaty) organic matter in the near-surface horizons and discrete plant root structures preserved in the lower parts of the sediment pile. Local concentrations of several hundreds ppm uranium occur in the peats, mainly around open, oxygenated root channels. Much higher levels are attained within the plant structures, apparently in cell material related to the water uptake system thus suggesting accumulation by the plant while living. Further study of live plant material from the site is needed to confirm this supposition which, if correct, would indicate that the transport and fixation mechanisms related to the soil-forming processes active on the sediments near the bottom of the pile were comparable to those of the present-day regime.

8. ACKNOWLEDGEMENTS

The authors wish to thank their colleagues in BGS for their help in the course of this research. In particular, Dr. P.J. Hooker is thanked for his helpful discussions and advice, Dr. T.K. Ball and Mr. P.D. Roberts are thanked for their help in field sampling and Dr. J.M. West is thanked for her useful discussions with regard to the microbiological and botanical features pertinent to this study. Staff at the Scottish Universities Research and Reactor Centre, East Kilbride, are thanked for carrying out the irradiations for fission track work. The Scottish Wildlife Trust is acknowledged for allowing access to the Needle's Eye site.

9. REFERENCES

Apps, M.J., Duke, M.J.M. and Stephens-Newsham, L.G. 1988. A study of radionuclides in vegetation on abandoned uranium tailings. Journal of Radioanalytical and Nuclear Chemistry, Articles, **123**, 133-147.

Basham, I.R. 1981. Some applications of autoradiographs in textural analysis of uranium-bearing samples - a discussion. Economic Geology, **76**, 994-997.

Basham, I. R., Ball, T.K., Beddoe-Stephens, B. and Michie, U.McL. 1982. Uranium-bearing accessory minerals in granite fertility: Methods of identification and evaluation. Uranium Exploration Methods, 385-397. Proceedings of Symposium, Paris, 1982. (OECD/IAEA).

Basham, I.R. & Hyslop E.K. 1989. Uranium location studies at the Needle's Eye Natural Analogue site - a preliminary account. Report Mineral Sciences Research Group, British Geological Survey, **WG/89/6R**.

Barnes, R.P. 1989. Geology of the Whithorn district, Memoir for 1:50 000 geological Sheet 2 (Scotland). British Geological Survey.

Beveridge, T.J., Meloche, J.D., Fyfe, W.S. and Murray, R.G.E. 1983. Diagenesis of metals chemically complexed to bacteria: laboratory formation of metal phosphates, sulphides, and organic condensates in artificial sediments. Applied and Environmental Microbiology, **45**, 1094-1108.

Capus, G. and Munier, C. 1978. Mise en évidence de fortes concentrations d'uranium dans les corps microbiens de micro-organisms actuels. Comptes Rendus de L'Academie des Sciences (Section D, Sciences Naturelles), **287**, 191-194.

Cronan, D.S. 1969. Recent sedimentation in the central north-eastern Irish Sea. Report, Institute of Geological Sciences, **69/8**.

Darnley, A.G., English, T.H., Sprake, O., Preece, E.R. and Avery, D. 1965. Ages of uraninite and coffinite from south-west England. Mineralogical Magazine, **34**, 159-176.

Degens, E.T. and Venugopalan, I. 1982. *In situ* metal-staining of biological membranes in sediments. Nature, **298**, 262-264.

Durrance, E.M. 1986. Radioactivity in geology: principles and applications. Ellis Horwood Ltd (publishers).

Eakin, P.A. 1989. Isotopic and petrographic studies of uraniferous hydrocarbons from around the Irish Sea Basin. Journal of the Geological Society, London, **146**, 663-673.

Esau, K. 1960. Anatomy of seed plants. Wiley & Sons (publishers).

Ferris, F.G. and Beveridge, T.J. 1985. Functions of bacterial cell surface structures. BioScience, **35**, 172-177.

Frondel, C. 1958. Systematic mineralogy of uranium and thorium. U.S. Geological Survey Bulletin, **1064**.

Gallagher, M.J., Michie, U.McL., Smith, R.T. and Haynes, L. 1971. New evidence of uranium and other mineralization in Scotland. Transactions of the Institute of Mining and Metallurgy, **80B**, 150-173.

Goodlet, G.A. 1970. Sands and gravels of the southern counties of Scotland. Report Institute of Geological Sciences, **70/4**.

Goldstein, J.I., Newbury, D.E., Echlin, P., Joy, D.C., Fiori, C. and Lifshin, E. 1981. Scanning Electron Microscopy and X-Ray Microanalysis: a text for Biologists, Materials Scientists, and Geologists. Plenum Press, New York and London (publishers).

Halliday, A.N., Stephens, W.E. and Harmon, R.S. 1980. Rb-Sr and O isotopic relationships in three zoned Caledonian granitic plutons, Southern Uplands, Scotland: evidence for varied sources and hybridisation of magmas. Journal of the Geological Society, London, **137**, 329-348.

Heinrich, E.W. 1958. Mineralogy and Geology of Radioactive Raw Materials. McGraw-Hill (publishers).

Horne, J. 1896. Explanation of Sheet 5. Memoirs of the Geological Survey, Scotland.

Hooker, P.J., MacKenzie, A.B., Scott, R.D., Ivanovich, M., Ball, T.K., Basham, I.R., Bloodworth, A.J. and Roberts, P.D. 1986. Natural analogues of radionuclide migration: reconnaissance study of sites (May 1985 - March 1986). Report Fluid Processes Research Group, British Geological Survey, **FLPU 86-6**.

Huggett, J.M. 1984. An SEM study of phyllosilicates in a Westphalian coal measures sandstone using back-scattered electron imaging and wavelength dispersive spectral analysis. Sedimentary Geology, **40**, 233-247.

Kleeman, J.D. and Lovering, J.F. 1967. Uranium distribution in rocks by fission track registration in Lexan plastic prints. Atomic Energy Australia, **10**, No.4, 3-8.

Krinsley, D.H., Pye, K. and Kearsley, A.T. 1983. Application of backscattered electron microscopy in shale petrology. Geological Magazine, **120**, 109-118.

Landais, P. 1989. Evidence for bacterial degradation of hydrocarbons in uranium deposits. Terra Nova, **1**, 163-171.

Magne, R., Berthelin, J.R. and Dommergues, Y. 1974. Solubilisation et insolubilisation de l'uranium des granites par des bacteries heterotrophes. Proceedings of Symposium on Formation of Uranium Ore Deposits, Athens, 1974. OECD/IAEA, 73-88.

Miller, J.M. and Taylor, K. 1966. Uranium mineralization near Dalbeattie, Kirkudbrightshire. Bulletin of the Geological Survey of Great Britain, **25**, 1-18.

Nakajima, A. and Sakaguchi, T. 1986. Selective accumulation of heavy metals by microorganisms. Applied Microbiology & Biotechnology, **24**, 59-64.

Palache, C., Berman, H. and Frondel, C. 1951. Dana's System of Mineralogy, Volume II: Halides, Nitrates, Borates, Carbonates, Sulphates, Phosphates, Arsenates, Tungstates, Molybdates, etc. Wiley & Sons, New York (publishers).

Parnell, J. 1988. Mineralogy of uraniferous hydrocarbons in Carboniferous-hosted mineral deposits, Great Britain. Uranium, **4**, 197-218.

Phillips, W.J., Fuge, R. and Phillips, N. 1981. Convection and crystallisation in the Criffel-Dalbeattie pluton. Journal of the Geological Society, London, **138**, 351-366.

Pye, K. and Krinsley, D.H. 1984. Petrographic examination of sedimentary rocks in the SEM using backscattered electron detectors. Journal of Sedimentary Petrology, **54**, 877-888.

Roberts, P.D., Ball, T.K., Hooker, P.J., MacKenzie, A.B., Milodowski, A.E. and Scott, R.D. 1988. A uranium geochemical study at the natural analogue site at Needle's Eye, SW Scotland. Proceedings, Materials Research Symposium (Berlin), **127**, 933-940.

Shaw, A.C., Lazell, S.K. and Foster, G.N. 1965. Photomicrographs of the flowering plant. Longmans (publishers).

Stephens, W.E., Whitley, J.E., Thirlwall, M.F. and Halliday, A.N. 1985. The Criffel zoned pluton: correlated behaviour of rare earth element abundances with isotopic systems. Contributions to Mineralogy and Petrology, **89**, 226-238.

Strong, G.E. and Milodowski, A.E. 1987. Aspects of diagenesis of the Sherwood Sandstones of the Wessex Basin and their influence on reservoir characteristics. in: Marshall, J.D. (editor). Diagenesis of Sedimentary Sequences. Geological Society Special Publication, **36**, 325-337.

European Communities — Commission

EUR 13279 — The location of uranium in source rocks and sites of secondary deposition at the Needle's Eye natural analogue site, Dumfries and Galloway

I. R. Basham, A. E. Milodowski, E. K. Hyslop, J. M. Pearce

Luxembourg: Office for Official Publications of the European Communities

1991 — IX, 56 pp., num. tab., fig. — 21.0 × 29.7 cm

Nuclear science and technology series

ISBN 92-826-2421-8

Catalogue number: CD-NA-13279-EN-C

Price (excluding VAT) in Luxembourg: ECU 6.25

The British Geological Survey has been conducting a coordinated research programme at the natural analogue site of Needle's Eye at Southwick on the Solway coast in south-west Scotland. This study of a naturally radioactive geochemical system has been carried out with the aim of improving our confidence in using predictive models of radionuclide migration in the geosphere. This report describes results of integrated mineralogical techniques which have been applied to the study of both the 'source-term' and sites of secondary accumulation of uranium. Pitchblende in a polymetallic-carbonate breccia vein exposed in ancient sea-cliffs is the main source of labile uranium although other uranium-bearing minerals present in the granodiorite and hornfelsed siltstone host-rocks present probable ancillary leachable sites. In keeping with the complex chemistry of the primary sulphide-rich mineralization, a large variety of secondary U minerals has been recorded among which arsenates and hydrous silicates appear to predominate. Uranium transported in groundwaters draining the cliffs has accumulated in organic-rich estuarine/intertidal mudflat sediments of Quaternary age. Charged particle track registration techniques have demonstrated convincingly the effectiveness of humified organic matter in retarding uranium transport and, coupled with scanning electron microscopy, have indicated the important role of living plants and bacteria in uranium uptake and concentration.

Venta y suscripciones • Salg og abonnement • Verkauf und Abonnement • Πωλήσεις και συνδρομές
Sales and subscriptions • Vente et abonnements • Vendita e abbonamenti
Verkoop en abonnementen • Venda e assinaturas

BELGIQUE / BELGIE

Moniteur belge / Belgisch Staatsblad
Rue de Louvain 42 / Leuvenseweg 42
1000 Bruxelles / 1000 Brussel
Tel. (02) 512 00 26
Fax 511 01 84
CCP / Postrekening 000 2005502-27

Autres distributeurs /
Overige verkooppunten

Librairie européenne/ Europese Boekhandel
Avenue Albert Jonnart 50 /
Albert Jonnartlaan 50
1200 Bruxelles / 1200 Brussel
Tel (02) 734 02 81
Fax 735 08 60

Jean De Lannoy
Avenue du Roi 202 /Koningslaan 202
1060 Bruxelles / 1060 Brussel
Tel. (02) 538 51 69
Télex 63220 UNBOOK B
Fax (02) 538 08 41

CREDOC
Rue de la Montagne 34 / Bergstraat 34
Bte 11 Bus 11
1000 Bruxelles / 1000 Brussel

DANMARK

J. H. Schultz Information A/S
EF-Publikationer
Ottiliavej 18
2500 Valby
Tlf. 36 44 22 66
Fax 36 44 01 41
Girokonto 6 00 08 86

BR DEUTSCHLAND

Bundesanzeiger Verlag
Breite Straße
Postfach 10 80 06
5000 Köln 1
Tel (02 21) 20 29 0
Fernschreiber:
ANZEIGER BONN 8 882 595
Fax 20 29 278

GREECE

G.C. Eleftheroudakis SA
International Bookstore
Nikis Street 4
10563 Athens
Tel. (01) 322 63 23
Telex 219410 ELEF
Fax 323 98 21

ESPANA

Boletín Oficial del Estado
Trafalgar, 27
28010 Madrid
Tel. (91) 44 82 135

Mundi-Prensa Libros, S.A.
Castelló, 37
28001 Madrid
Tel. (91) 431 33 99 (Libros)
431 32 22 (Suscripciones)
435 36 37 (Dirección)
Télex 49370 MPLI-E
Fax (91) 575 39 98

Sucursal:

Librería Internacional AEDOS
Consejo de Ciento, 391
08009 Barcelona
Tel. (93) 301 86 15
Fax (93) 317 01 41

Llibreria de la Generalitat de Catalunya
Rambla dels Estudis , 118 (Palau Moja)
08002 Barcelona
Tel. (93) 302 68 35
302 64 62
Fax 302 12 99

FRANCE

Journal officiel
Service des publications des Communautés européennes
26, rue Desaix
75727 Paris Cedex 15
Tél. (1) 40 58 75 00
Fax (1) 40 58 75 74

IRELAND

Government Publications Sales Office
Sun Alliance House
Molesworth Street
Dublin 2
Tel. 71 03 09

or by post

Government Stationery Office
EEC Section
6th floor
Bishop Street
Dublin 8
Tel. 78 16 66
Fax 78 06 45

ITALIA

Licosa Spa
Via Benedetto Fortini, 120/10
Casella postale 552
50125 Firenze
Tel. (055) 64 54 15
Fax 64 12 57
Telex 570466 LICOSA I
CCP 343 509

Subagenti:

Libreria scientifica Lucio de Biasio - AEIOU
Via Meravigli, 16
20123 Milano
Tel. (02) 80 76 79

Herder Editrice e Libreria
Piazza Montecitorio, 117-120
00186 Roma
Tel. (06) 679 46 28 679 53 04

Libreria giuridica
Via XII Ottobre, 172 R
16121 Genova
Tel. (010) 59 56 93

GRAND-DUCHÉ DE LUXEMBOURG

Abonnements seulement
Subscriptions only
Nur fur Abonnements

Messageries Paul Kraus
11, rue Christophe Plantin
2339 Luxembourg
Tél. 499 88 88
Télex 2515
Fax 499 88 84 44
CCP 49242-63

NEDERLAND

SDU Overheidsinformatie
Externe Fondsen
Postbus 20014
2500 EA 's-Gravenhage
Tel. (070) 37 89 911
Fax (070) 34 75 778

PORTUGAL

Imprensa Nacional
Casa da Moeda, EP
Rua D. Francisco Manuel de Melo, 5
P-1092 Lisboa Codex
Tel. (01) 69 34 14

Distribuidora de Livros Bertrand, Ld.ª
Grupo Bertrand, SA
Rua das Terras dos Vales, 4-A
Apartado 37
P-2700 Amadora Codex
Tel. (01) 49 59 050
Telex 15798 BERDIS
Fax 49 60 255

UNITED KINGDOM

HMSO Books (PC 16)
HMSO Publications Centre
51 Nine Elms Lane
London SW8 5DR
Tel. (071) 873 9090
Fax GP3 873 8463
Telex 29 71 138

Sub-agent:

Alan Armstrong Ltd
2 Arkwright Road
Reading, Berks RG2 0SQ
Tel. (0734) 75 18 55
Telex 849937 AAALTD G
Fax (0734) 75 51 64

ÖSTERREICH

Manz'sche Verlags- und Universitätsbuchhandlung
Kohlmarkt 16
1014 Wien
Tel. (0222) 531 61-0
Telex 11 25 00 BOX A
Fax (0222) 531 61-81

SVERIGE

BTJ
Box 200
22100 Lund
Tel. (046) 18 00 00
Fax (046) 18 01 25

SCHWEIZ SUISSE SVIZZERA

OSEC
Stampfenbachstraße 85
8035 Zurich
Tel. (01) 365 51 51
Fax (01) 365 54 11

MAGYARORSZÁG

Agroinform
Kozpont:
Budapest I., Attila ut 93. H-1012

Levélcím:
Budapest, Pf.: 15 H-1253
Tel. 36 (1) 56 82 11
Telex (22) 4717 AGINF H-61

POLAND

Business Foundation
ul. Wspólna 1 3
PL-00-529 Warszawa
Tel. 48 (22) 21 99 93 21 84 20
Fax 48 (22) 28 05 49

YUGOSLAVIA

Privredni Vjesnik
Bulevar Lenjina 171/XIV
11070 - Beograd
Tel. 123 23 40

TURKIYE

Pres Dagitim Ticaret ve sanayi A.Ş.
Narlibahçe Sokak No. 15
Cağaloglu
Istanbul
Tel. 512 01 90
Telex 23822 DSVO-TR

AUTRES PAYS
OTHER COUNTRIES
ANDERE LÄNDER

Office des publications officielles des Communautés européennes
2, rue Mercier
L-2985 Luxembourg
Tél. 49 92 81
Telex PUBOF LU 1324 b
Fax 48 85 73
CC bancaire BIL 8-109/6003/700

CANADA

Renouf Publishing Co. Ltd
Mail orders — Head Office:
1294 Algoma Road
Ottawa, Ontario K1B 3W8
Tel. (613) 741 43 33
Fax (613) 741 54 39
Telex 0534783

Ottawa Store:
61 Sparks Street
Tel. (613) 238 89 85

Toronto Store:
211 Yonge Street
Tel. (416) 363 31 71

UNITED STATES OF AMERICA

UNIPUB
4611-F Assembly Drive
Lanham, MD 20706-4391
Tel. Toll Free (800) 274 4888
Fax (301) 459 0056

AUSTRALIA

Hunter Publications
58A Gipps Street
Collingwood
Victoria 3066

JAPAN

Kinokuniya Company Ltd
17-7 Shinjuku 3-Chome
Shinjuku-ku
Tokyo 160-91
Tel. (03) 3439-0121

Journal Department
PO Box 55 Chitose
Tokyo 156
Tel. (03) 3439-0124

15

CD-NA-13279-EN-C

NOTICE TO THE READER

All scientific and technical reports published by the Commission of the European Communities are announced in the monthly periodical **'euro abstracts'**. For subscription (1 year: ECU 92) please write to the address below.

Price (excluding VAT) in Luxembourg: ECU 6.25

OFFICE FOR OFFICIAL PUBLICATIONS
OF THE EUROPEAN COMMUNITIES

L-2985 Luxembourg

ISBN 92-826-2421-8

9 789282 624210